pubs.acs.org/JACS

Article

Pools of Independently Cycling Inositol Phosphates Revealed by Pulse Labeling with ¹⁸O-Water

Geun-Don Kim,[#] Guizhen Liu,[#] Danye Qiu, Maria Giovanna De Leo, Navin Gopaldass, Jacques Hermes, Jens Timmer, Adolfo Saiardi, Andreas Mayer,* and Henning Jacob Jessen*



Cite This: J. Am. Chem. Soc. 2025, 147, 17626-17641



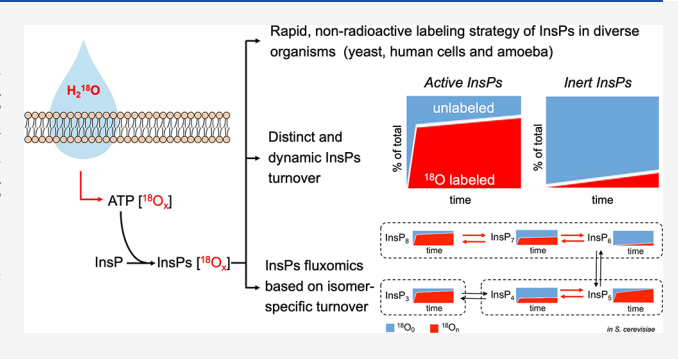
ACCESS

III Metrics & More

Article Recommendations

SI Supporting Information

ABSTRACT: Inositol phosphates control many central processes in eukaryotic cells including nutrient availability, growth, and motility. Kinetic resolution of a key modulator of their signaling functions, the turnover of the phosphate groups on the inositol ring, has been hampered by slow uptake, high dilution, and constraining growth conditions in radioactive pulse-labeling approaches. Here, we demonstrate a rapid (seconds to minutes) and nonradioactive labeling strategy of inositol polyphosphates through ¹⁸O-water in yeast, human cells, and amoeba, which can be applied in any media. In combination with capillary electrophoresis and mass spectrometry, ¹⁸O-water labeling simultaneously dissects the in vivo phosphate group dynamics of a broad spectrum of even



rare inositol phosphates. The good temporal resolution allowed us to discover vigorous phosphate group exchanges in some inositol polyphosphates and pyrophosphates, whereas others remain remarkably inert. We propose a model in which the biosynthetic pathway of inositol polyphosphates and pyrophosphates is organized in distinct, kinetically separated pools. While transfer of compounds between those pools is slow, each pool undergoes rapid internal phosphate cycling. This might enable the pools to perform distinct signaling functions while being metabolically connected.

1. INTRODUCTION

Water-soluble cytosolic inositol phosphates (InsPs) can be synthesized by rearrangement of glucose-6-phosphate to inositol-3-phosphate or emanate from the hydrolysis of inositol lipids (Figure 1). Inositol-containing metabolites have key signaling roles in eukaryotic cells. Phosphatidylinositol lipids (PtdInsPs or simply PIPs) determine the identity of organelles and organize vesicular traffic between them. The biologically occurring species with phosphate groups in different positions of the inositol headgroup are important to cell polarity, movement and mechanotransduction, the release of growth factors, neurotransmitters, and hormones.² The cytosolic or water-soluble InsPs have equally diverse and important signaling functions, including DNA stability, RNA transport, transcriptional control, MAP kinase signaling, maintaining energy homeostasis, and many others.³⁻⁵ Inositol pyrophosphates (PP-InsPs), the most highly phosphorylated watersoluble InsPs, which contain diphosphate groups, link phosphate homeostasis to adenosine triphosphate (ATP) levels across species, in part by signaling via SPX (Syg1/ Pho81/Xpr1) domain-containing proteins. 6-12

In many of the processes mentioned above, InsPs and PtdInsPs are interconverted, leading to alterations of the number and/or the positioning of their phosphate groups. Measuring the steady-state levels of InsPs and PP-InsPs has

usually been achieved by strong anion exchange-high-performance liquid chromatography (SAX-HPLC) after metabolic labeling with ³H or ¹⁴C-inositol, but this is a lengthy process that requires 24 h in yeast to several days in mammalian cells under constraining growth conditions. 13 More recently, capillary electrophoresis-mass spectrometry (CE-MS) has been introduced to monitor absolute InsP and PP-InsP levels, $^{14-17}$ and stable isotope $^{13}\mathrm{C}$ labeling with glucose and inositol has revealed alternative pathways of soluble InsP synthesis from membrane lipids or glucose (Figure 1). 15,18 Although these approaches can be used to separate and quantify the steady-state levels of InsPs and PP-InsPs, the fast dynamics of the interconversion of the phosphate groups in cells has remained difficult to capture. This is in large part due to inherent limitations and complexity of the pulse-labeling approaches with radiolabeled tracers, which have so far been necessary for such analyses.19

Received: November 15, 2024 Revised: May 8, 2025 Accepted: May 8, 2025 Published: May 15, 2025





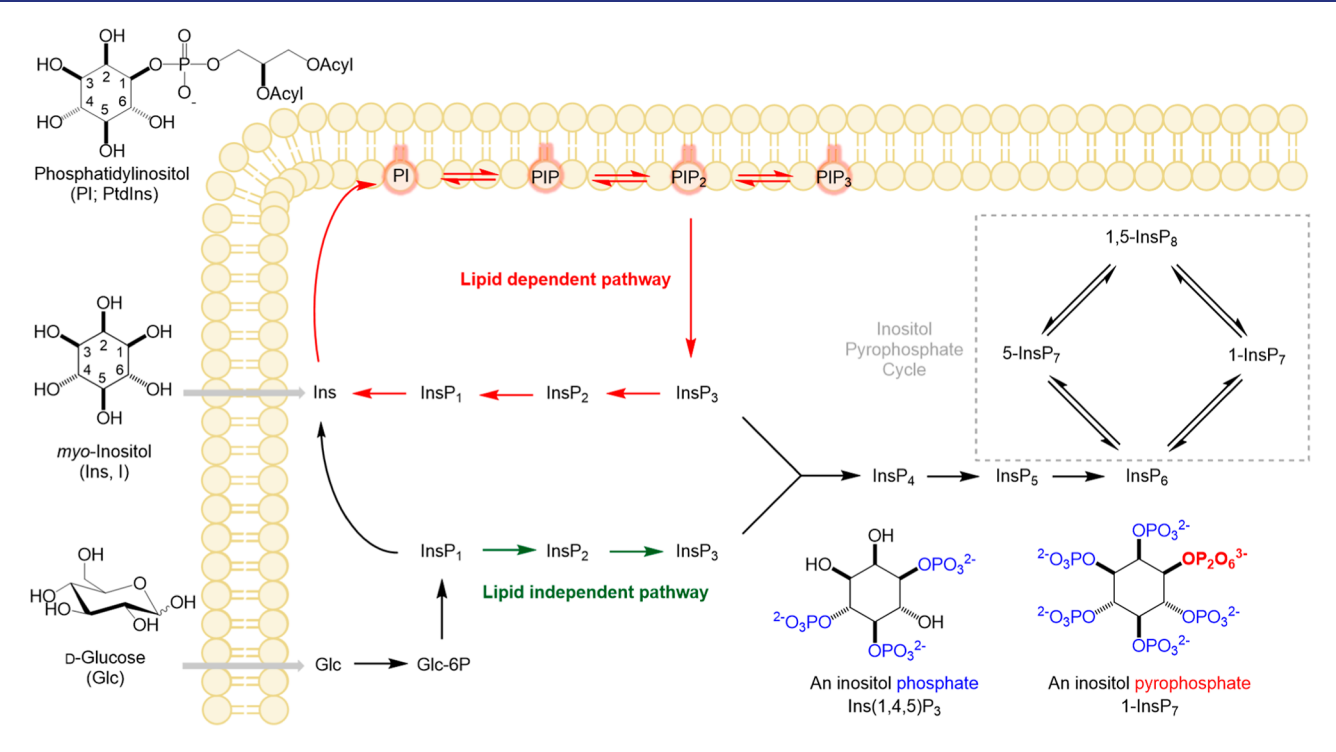


Figure 1. Pathways for synthesis of lipidic and generic soluble inositol phosphates. Inositol can either be taken up by cells or synthesized from glucose after uptake and phosphorylation. Cytosolic inositol phosphates are generated from $PtdInsP_2$ (PIP2) through phospholipase C (PLC), generating diacylglycerol and $InsP_3$. In mammalian cells, an additional lipid-independent pathway can generate $InsP_3$ directly from glucose. Proward phosphorylation by kinases up to $InsP_8$ is possible while phosphatases remove the phosphate groups, generating lower phosphorylated forms. The balance between kinases and phosphatases will likely occur at different rates controlled by metabolic and/or signaling inputs. Therefore, we can envisage an InsP network constantly turning over, harmonizing the steady-state concentrations of the different metabolites.

Inositol phosphates can be labeled through feeding the cells with radiolabeled inositol or by adding isotope-labeled phosphate.¹³ Inositol uptake is slow, and labeling is usually performed to isotopic equilibrium, involving a culture in inositol-depleted media over several generations. Moreover, inositol can be synthesized by cells from glucose, which leads to unlabeled inositol that cannot be traced. 14,18 32P labeled inositol phosphate enables us to study the sequential addition of phosphate but is limited because even after 40 min of labeling, ATP does not reach isotopic equilibrium. 21-23 Phosphate labeling is also comparatively slow because it relies on uptake through plasma membrane transporters. It is subjected to isotopic dilution both in the medium, where phosphate is an essential macronutrient, and in the cell, which has cytosolic phosphate concentrations of up to 20 mM²⁴ and storage pools for phosphate. Furthermore, Pi utilization, and thereby the ability to label the internal P_i pool through P_i uptake, is strongly influenced by biosynthesis and cell growth, which change as a function of the culture conditions.

While steady-state levels of metabolites themselves are an important information, the dynamic turnover of metabolites in this steady state, the metabolic flux, reflects the activity of a metabolic pathway. Flux provides additional information about the metabolic state and can constitute a signal for the cell. Can help us understand how a steady-state concentration is maintained and how quickly a system can adjust to perturbations. For example, the use of NaF as metabolic trap to block metabolic fluxes depending on phosphatases revealed dynamic phosphorylation of the abundant InsP₆ (50–100 μ M) into scarce PP-InsPs (0.1–2 μ M), with a turnover of ca. 50% of the whole InsP₆ pool within 1 h. Si

Measuring the dynamic turnover of phosphorylated metabolites should ideally rely on direct labeling of the phosphate groups. This can be achieved by using isotopes. For phosphorus, only radioactive nuclides are available. Furthermore, phosphorus can be absorbed by cells only in the form of organic or inorganic phosphate (Pi). The uptake process can be quite slow, rendering it difficult to monitor rapid processes, as, for example, even after 40 min radioactive Pi treatment of duckweed, ATP is not labeled to equilibrium.²² Another option of labeling the phosphate group is by stable isotope labeling using ¹⁸O-enriched water. ^{30,32-35} Water enters cells within seconds. It is incorporated into P, by hydrolytic enzymatic reactions. A purely chemical exchange of P_i is inefficient.^{30,36} Hydrolysis occurs vigorously on cellular nucleotides, as exemplified by ATP, for which the entire cellular pool can turn over in seconds. 30,37 This rapid cycling entrains a similarly rapid introduction of 18O into the hydrolytic product, Pi.

The incorporation of 18 O into ATP (9 oxygens are exchangeable via different enzymatic mechanisms) has been studied extensively using direct 31 P nuclear magnetic resonance (NMR) approaches and liquid chromatography—mass spectrometry, as well as by an indirect gas chromatography—mass spectrometry approach. 25,38 Due to the inherently low sensitivity of NMR, this approach will not be effective to monitor scarce signaling molecules with high turnover rates. Of particular interest for phosphotransfer reactions is the appearance of the isotope label in the γ -phosphate of ATP as this is the most readily transferable phosphate group. In rat hearts, for example, the γ -phosphate in every ATP is turned over 34 times per minute, the β -phosphate 12 times, and the α -phosphate only once a minute. 25 ATP-synthase can incorpo-

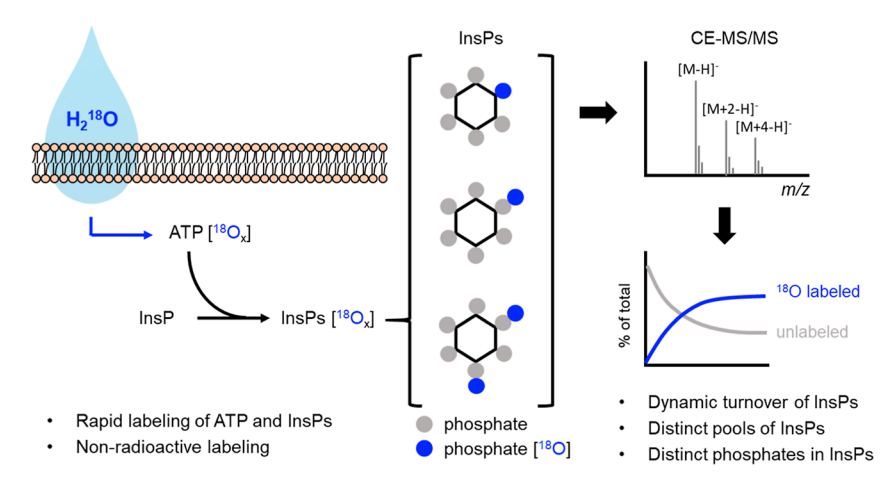


Figure 2. Workflow for the analysis of cellular ¹⁸O labeled ATP and InsP pools through ¹⁸O-water labeling, combined with CE-MS analysis.

rate ¹⁸O from ¹⁸O-water even multiple times into ATP before releasing its product into the cell. These studies have consistently demonstrated very rapid incorporation of ¹⁸O labels, particularly in the γ -phosphate. Earlier experiments with ¹⁸O-water have also underpinned the existence of different compartmentalized ATP pools (metabolic and nonmetabolic), which vary with cell types and physiological states.³⁰ While ¹⁸O-labeling was exploited for a limited number of analyses of ATP turnover and labeled synthetic ¹⁸O ATP has been used in phosphoproteomics, 40,41 the potential of an extension of this concept to other areas of phosphorylated metabolites received only limited attention. Recently, a study has shown incorporation of ¹⁸O labels into the PtdInsPs phosphate diester after incubation of mammalian cells with ¹⁸O-water. ^{34,42} Furthermore, the advent of new chemical synthesis approaches made ¹⁸O labeled reference compounds available, enabling ionization and fragmentation studies to improve assignments and quantifications of inositol phosphates.4

Here, we use pulse-labeling to explore the turnover of inositol polyphosphates of yeast, amoeba, and mammalian cells. Since these are in large part low-abundance metabolites (nanomolar to low micromolar concentration), we rely on the sensitivity and separation power of capillary electrophoresis coupled to both triple quadrupole (QQQ) and quadrupole time-of-flight (qTOF) mass spectrometry for their analysis, of which the first one is more sensitive. Our in vivo approach is based on the rapid permeation of ¹⁸O water into cells and on the extremely rapid turnover of the cellular P_i through nucleotide hydrolysis.^{37,46} Our results provide an entry point into coupled InsP and PP-InsP fluxomics, revealing unexpectedly high turnover rates of some metabolites, metabolic lethargy of others, selective impact of applied conditions/ knockouts on ¹⁸O labeling kinetics, and, most notably, the existence of several independently cycling InsP pools (workflow shown in Figure 2).

2. RESULTS

2.1. Rapid ¹⁸O Labeling of ATP in Yeast. To label yeast cells, cultures that were logarithmically growing in SC (synthetic complete) medium were transferred to the same SC medium made with 50% ¹⁸O-water. 50% ¹⁸O-water suffices to label the entire pool of P_i almost quantitatively because, in isotopic equilibrium, the probability of P_i remaining with four unlabeled oxygen atoms is equal to 1/16 (6%). In this medium, P_i is the sole source of phosphate. At different time

points, aliquots of the culture were extracted with perchloric acid, ^{47,48} and the extracts were analyzed by CE-MS (Figure 2). The number of labels was assigned by combination of internal standards and high-resolution qTOF mass spectrometry (Figure 3A). Already at the first time point taken, after 1 min, ATP with one-four ¹⁸O atoms was detected (Figure 3A). Labeling proceeded rapidly, even at 20 °C, reaching up to seven ¹⁸O labels after 60 min. The ¹⁸O labels also rapidly penetrated the InsPs, which could be analyzed from the same extracts used for nucleotide analytics. The gradual incorporation of multiple labels poses a problem for rare analytes because the already low abundance of ions is now distributed over all isotopologues. This renders the MS analysis of rare analytes challenging, such as InsP₅ and inositol pyrophosphates (InsP₇ and InsP₈), and complicates the detection of analytes with a large number of ¹⁸O atoms. To try to quantify all these rare analytes, CE-MS with a triple quadrupole system (CE-QQQ) in multiple reaction monitoring (MRM) mode was employed because it offers higher sensitivity than the qTOF system.

Specified transitions from precursor to product ions were optimized by the MassHunter optimizer with injection of standards to maximize the product ion signal. The ion at m/z408.0117, one of the major fragmented ions found corresponding to $[M - H - H_3PO_4]^-$ for unlabeled ATP, was chosen as the product ion (Figure S1). An unexpected oxygen exchange (scrambling) on ATP was detected through analysis of the synthetic control compound $\gamma^{-18}O_2$ -ATP⁴⁴—which carries two defined ^{18}O as nonbridging oxygens of the γ -phosphate (Figure S2) with >99% $^{18}O_2/^{16}O_2$ ratio. However, its MS2 fragmentation showed partial scrambling of ¹⁸O in the gas phase under these conditions, i.e., we observed monolabeled γ-phosphate and monolabeled adenosine diphosphate (ADP). 49% of single ¹⁸O scrambles and 16% of double ¹⁸O scrambles were observed (Figure S2). It is mechanistically conceivable that such an exchange of oxygens might occur through a reversible ping-pong gas-phase reaction involving metaphosphates.

Scrambling was also observed when synthetic [$^{18}O_2$] 5-InsP $_7$ was employed, 43 which was only labeled on the nonbridging oxygens in the β -phosphate (Supplementary Figure S3). Optimization of the MS parameters with synthetic γ - $^{18}O_2$ -ATP and [$^{18}O_2$] 5-InsP $_7$ did not reduce the observed scrambling. Therefore, to accurately count the numbers of ^{18}O labels in the analytes and avoid an underestimation of the

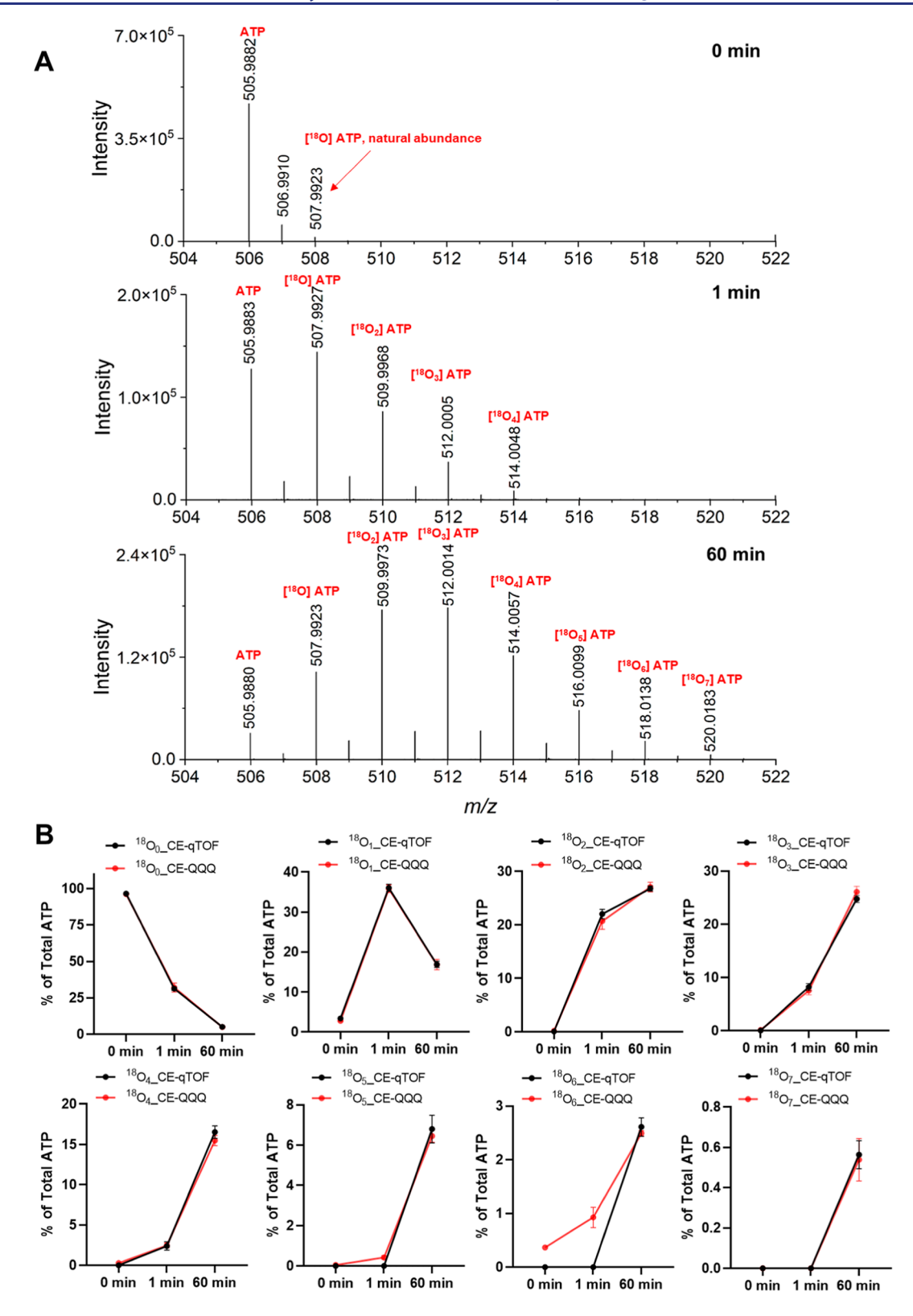


Figure 3. (A) qTOF MS analysis of ATP. The analysis reveals the kinetics of ¹⁸O incorporation into ATP at different exchangeable positions. Wild-type yeast cells were grown in SC medium at 20 °C to slow down the incorporation. At the 0 min time point, the medium was changed to SC medium prepared with 50% ¹⁸O-water. Samples were harvested at different time points (1 and 60 min), extracted with perchloric acid and TiO₂, and analyzed by qTOF mass spectrometry. Theoretical [M-H]⁻ for ATP, [¹⁸O] ATP, [¹⁸O] ATP, [¹⁸O₃] ATP, [¹⁸O₄] ATP, [¹⁸O₅] ATP, [¹⁸O₆] ATP, and [¹⁸O₇] ATP are 505.9885, 507.9927, 509.9970, 512.0012, 514.0055, 516.0097, 518.0139, and 520.0182, respectively. (B) The incorporation of ¹⁸O into ATP was analyzed at 0, 1, and 60 min using CE-qTOF (MS1) and CE-QQQ (MRM) methods. The means of 3 samples with standard deviation are shown.

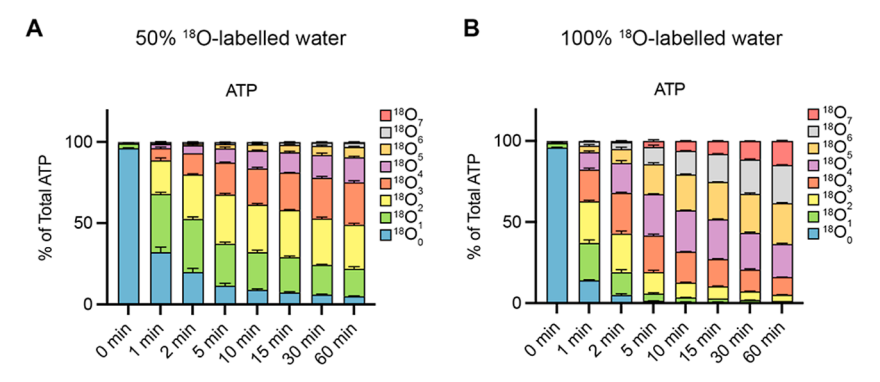


Figure 4. Kinetics of ¹⁸O entry into ATP of yeast under steady-state conditions. Time-dependent formation of ATP isotopologues in yeast with different numbers of ¹⁸O atoms studied by CE-QQQ with wide mass resolution. Wild-type yeast cells were grown logarithmically in SC medium at 20 °C. At the 0 min time point, the medium was changed to SC medium prepared with A 50% or B 100% of ¹⁸O-labeled water (99% enrichment). After further incubation at 20 °C for the indicated periods of time, cells were extracted with perchloric acid and TiO₂. The graphs show the fractions of ATP that carried the indicated numbers of ¹⁸O at any position. The means of 3 samples with standard deviation are shown.

extent of labeling, scrambled product ions had to be considered when using the MRM transitions by CE-QQQ. For example, the observed scrambled product ions, such as ($^{18}O_2$ ATP-H-H₃PO₂ $^{18}O_2$)⁻, ($^{18}O_2$ ATP-H-H₃PO₃ ^{18}O)⁻, and ($^{18}O_2$ ATP-H-H₃PO₄)⁻, were summed to calculate the total ¹⁸O₂ ATP (Table S3). We also considered the scrambled product ions for InsPs. For example, the observed scrambled product ions (${}^{18}O_2$ InsP₇-2H-H₃PO₄)²⁻, (${}^{18}O_2$ InsP₇-2H- $H_3PO_3^{18}O)^{2-}$, and $(^{18}O_2 \text{ InsP}_{7-}2H-H_3PO_2^{18}O_2)^{2-}$ were recorded with the same precursor ion, ¹⁸O₂ InsP₇ (Table S4). The MRM transitions for all analytes are detailed in Tables S3-S8. To assess whether our consideration of all scrambled product ions in the CE-QQQ method allows for accurate measurements of ¹⁸O incorporation ratios, we compared the quantitative results at 0, 1, and 60 min obtained using CE-qTOF (MS1 level, where no scrambling occurs) and CE-QQQ (MRM, accounting for all scrambled product ions). As shown in Figure 3B, there is excellent agreement between the results from CE-qTOF and CE-QQQ, except for ¹⁸O₆ ATP. The slight deviation (less than 1%) observed at 1 min for ¹⁸O₆ incorporation is due to the lower sensitivity of CE-qTOF in detecting 18O6 ATP at 1 min, whereas CE-QQQ demonstrates a higher sensitivity for the detection. This shows that our CE-QQQ method accurately and sensitively reveals ¹⁸O incorporation. In summary, using synthetic ¹⁸O labeled ATP and InsP7 allowed us to identify the scrambling of ¹⁸O during the MS/MS fragmentation in the gas phase and to optimize the MRM transitions and accurately count the numbers of ¹⁸O labels on ATP and InsPs by CE-QQQ.

2.2. Rapid Pulse-Labeling Resolves Separate, Cycling Pools of Soluble Inositol Polyphosphates in Yeast. Using our previously described CE-MS method, ¹⁴ we monitored the time course of ¹⁸O incorporation from ¹⁸O-water into ATP by CE-QQQ. Already after 1 min at 20 °C more than 68% of the ATP pool was labeled (Figure 4A, for a representative example of extracted ion electropherograms see Figure S4). The ATP labeling tended to be even faster and was shifted to larger numbers of total ¹⁸O incorporation when 100% ¹⁸O-water was used in the culture medium (Figure 4B), which was, however, avoided for cost reasons.

ATP does not undergo spontaneous ^{16/18} oxygen exchange in ¹⁸ O-water. Further addition of inositol hexakisphosphate kinase (IP6K1), which could potentially catalyze an exchange, did not have any effect either (Figure S5).

The ¹⁸O labels rapidly appeared in InsPs and PP-InsPs, which could be analyzed from the same extracts as used for ATP analytics by CE-MS, although measuring low-abundance metabolites (e.g., 5-InsP₇ and 1,5-InsP₈) has challenges due to mass resolution constraints and isotopic interference. These ¹⁸O labels result neither from spontaneous ^{16/18}oxygen exchange in the presence of ¹⁸O-water (Figure S6), nor from extraction of InsPs and PP-InsPs (Figure S7). They are also not transferred by inositol hexakisphosphate kinase in the absence of ¹⁸O-ATP (Figures S8 and S9). Our measurements yielded ¹⁸O signals in InsP₇ and InsP₈ that were already above the expected natural abundance of ¹⁸O at the 0 min time point. Since the isotope frequency of ¹⁸O is 0.2% and inositol polyphosphates are very oxygen-rich molecules (e.g., 27 oxygens for InsP7), this leads to an expected fraction of ca. 5-6% of these compounds carrying at least one 18 O. Our analytical protocol overestimates (from ca. 5% to 15% at the 0 min time point) this expected value only for InsP₇ and InsP₈, due to overlap with isotopic peaks of unlabeled PP-InsPs when using the wide mass resolution (full-width at half-maximum of 1.2 Da, ± 0.6 Da mass error) of the quadrupole. We had to choose wide mass resolution in these experiments to attain the sensitivity needed to quantify ¹⁸O labeled InsP₇ and InsP₈, which are very low-abundance metabolites. Wide mass resolution can separate major isotopic clusters, such as carbon-based compounds dominated by ¹²C and ¹³C, referred to as M and M+1. In the case of InsP7 and InsP8, doubly charged precursor ions and product ions were detected, resulting in a skewing of the expected value from 5 to 15% at the 0 min time point. By contrast, the example of ATP representing analytes with singly charged precursor or product ions showed an excellent agreement between the results of unit mass resolution and wide mass resolution. This indicates that almost no skewing in the measurement of singly charged precursor or product ions occurs (Figures S10 and S11).

The skewing in $InsP_7$ and $InsP_8$ quantification could potentially be corrected by performing unit mass resolution measurements, which is specified to have only ± 0.35 Da mass error (Figure S12). However, unit mass resolution, which results in an approximate 3-fold reduction of the signal intensity compared to wide mass resolution, was not sufficiently sensitive to quantify ^{18}O labeled $InsP_8$. With this information, we reanalyzed ^{18}O labeled $InsP_7$ in unit-mass resolution (Figures 5B and S17B) under optimal conditions

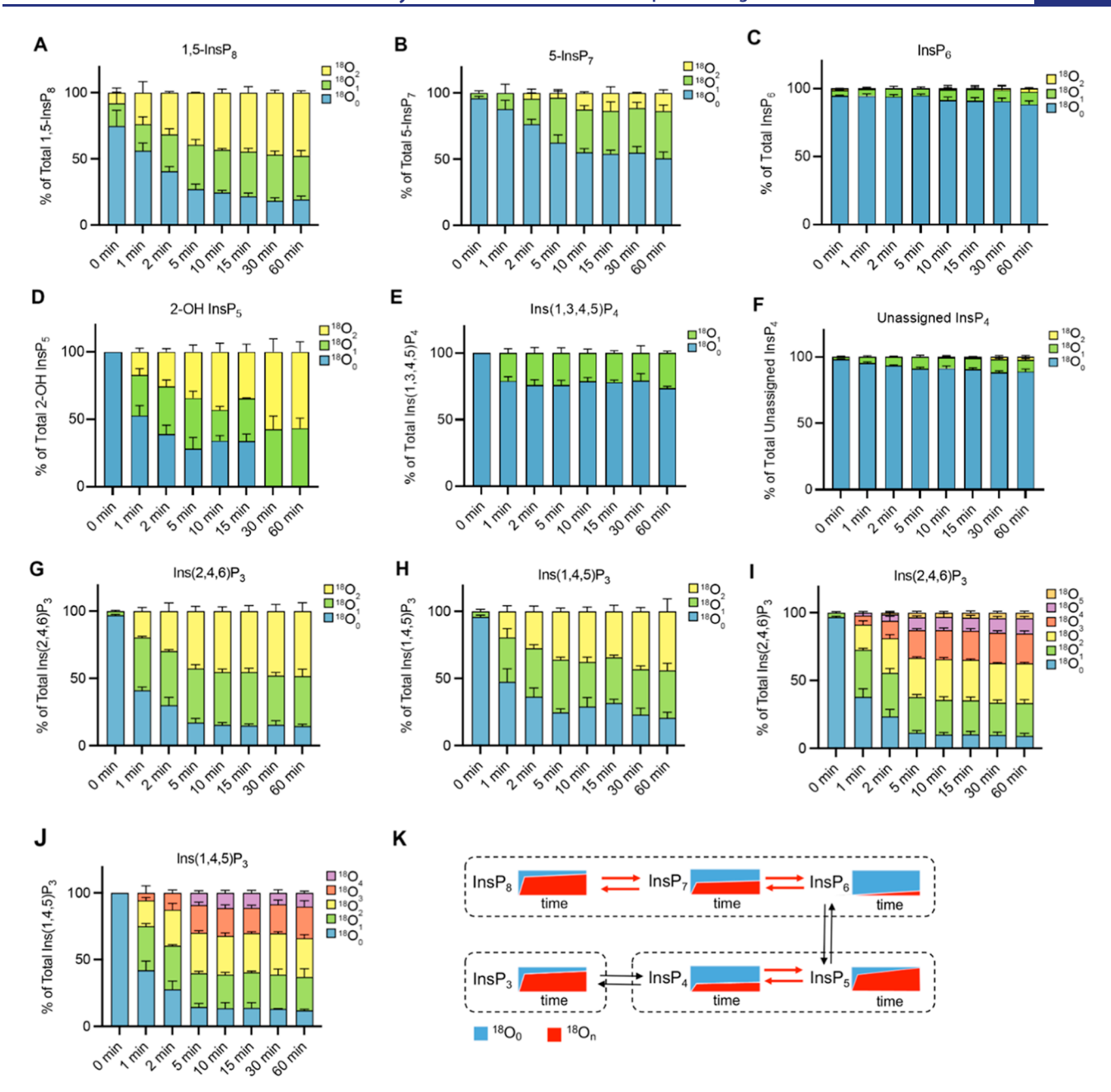


Figure 5. Kinetics of ¹⁸O entry into soluble InsPs of yeast under steady-state conditions. Wild-type yeast cells were grown logarithmically in SC medium at 20 °C. The medium was changed to SC medium prepared with 50% of ¹⁸O-labeled water. After further incubation at 20 °C for the indicated periods of time, cells were extracted with perchloric acid and TiO₂ and analyzed by CE-QQQ or qTOF. Note that the levels of 1-InsP₇ in these samples were too low to be reliably detected. The means of 3 samples with standard deviation is shown, representing (A) 1,5-InsP₈, (B) 5-InsP₇, (C) InsP₆, (D) 2-OH-InsP₅, (E) Ins(1,3,4,5,)P₄, (F) unassigned InsP₄, (G) Ins(2,4,6)P₃, (H) Ins(1,4,5)P₃, (IJ) higher numbers of ¹⁸O incorporation into InsP₃ were observed by CE-qTOF of samples as in (G,H,K). Proposed pathways of interconversion. Rapid interconversion of metabolites is indicated by red arrows, and slow interconversion by black arrows. CE-QQQ with wide mass resolution was used in (A,C,D,E,F,G,H), and CE-QQQ with unit mass resolution was used in (B).

(first-class capillary cut, freshly prepared sheath liquid, and fresh background electrolyte). This approach still did not enable the measurement of $InsP_8$, which is therefore reported in wide mass resolution with the expected skewing (Figures 5A and S17A).

To estimate whether the described skewing effect changed its magnitude during the time course, mixtures of synthetic ¹⁸O₂ 5-InsP₇ and unlabeled 5-InsP₇ with different compositions were prepared and analyzed by CE-QQQ using wide mass resolution. Raising the concentration of the ¹⁸O₂ 5-InsP₇

reduces the skewing of ¹⁸O 5-InsP₇ from 10% to less than 3% (Figure S13). Also, in our time course experiments, the effect is largest at the zero time point (ca. 10–20%) and declines during increasing incorporation of ¹⁸O labels (Figure S15), which made a simple subtraction to the expected zero-time point value problematic. A 2-fold change in the concentration of ¹⁸O₂ 5-InsP₇ decreased skewing by 2%. Comparison of the 5-InsP₇ results based on unit mass resolution with wide mass resolution results in yeast samples demonstrate a similar trend in ¹⁸O labeling overtime (Figures

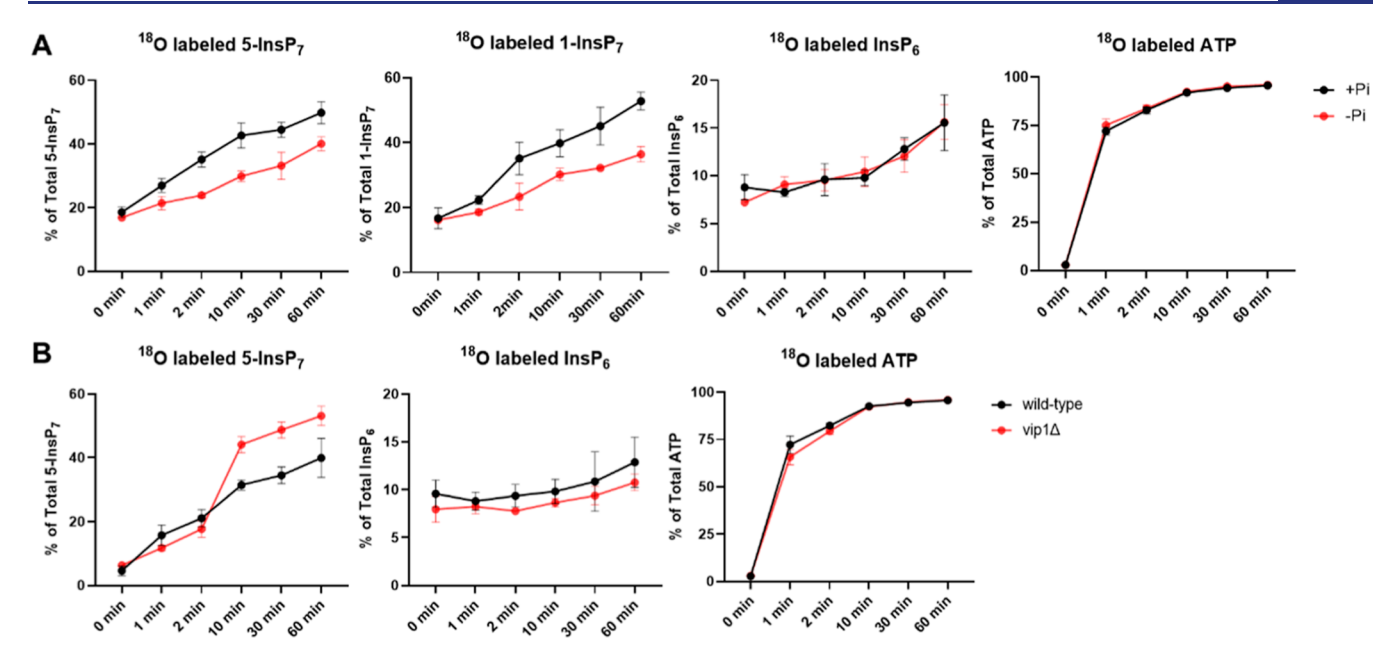


Figure 6. Kinetics of 18 O entry into soluble InsPs and ATP of yeast under different Pi conditions and in vip1 Δ mutant. Yeast cells grown in P_i-rich medium were transferred to P_i-rich or P_i-free media containing 50% 18 O-labeled water, and aliquots were analyzed at the indicated time points following the transfer. Cells were extracted with perchloric acid and TiO₂ and analyzed by CE-QQQ. The means of 3 samples with standard deviation is shown. (A) 18 O labeled 5-InsP₇ (sum of 18 O₁ and 18 O₂), 1-InsP₇ (sum of 18 O₁ and 18 O₂), InsP₆ (sum of 18 O₁ and 18 O₂), and ATP (sum of 18 O₇) in the wild-type yeast under different Pi conditions. ATP was measured by CE-QQQ with unit mass resolution, whereas the others were measured by CE-QQQ with wide mass resolution. (B) 18 O labeled 5-InsP₇ (sum of 18 O₁ and 18 O₂), InsP₆ (sum of 18 O₁ and 18 O₂), and ATP (sum of 18 O₁ to 18 O₇) in the wild-type and vip1 Δ mutant under P₁-rich condition. ATP and 5-InsP₇ were measured by CE-QQQ with unit mass resolution, whereas the others were measured by CE-QQQ with wide mass resolution.

S14 and S15), indicating the skewing does not impact the trend used to assess the dynamic turnover of phosphorylated InsPs and PP-InsPs in this study. In summary, ¹⁸O labeling of the inositol pyrophosphates InsP₇ and InsP₈ is moderately overestimated in the wide mass resolution approach. This error must be accepted as a trade-off for attaining the enhanced sensitivity that is necessary for analyzing ¹⁸O transfer to very low-abundance PP-InsPs, such as InsP₈. Consequently, the following results were obtained using wide mass resolution CE-QQQ, except for 5-InsP₇ in yeast (Figures 5B and S17B).

Next, the turnover of the inositolpyrophosphates, particularly 5-InsP₇ and 1,5-InsP₈, was studied in cells under constant nutrient availability. When the cells were transferred from unlabeled culture medium into medium of the same composition but made from 50% ¹⁸O-water, 12% of 5-InsP₇ and 44% of 1,5-InsP₈ acquired one or two ¹⁸O labels already within 1 min (Figure 5A,B, for representative examples of extracted ion electropherograms see Figure S16). For 1,5-InsP₈, this led to 78% labeling of the pool within 15 min and remained almost constant thereafter. Labeled 5-InsP7 attained 46% within the first 15 min, which then slowly increased for the rest of the 60 min incubation period (50% of labeled 5-InsP₇). This suggests the existence of at least two pools of 5-InsP₇, one resting static and the other one turning over very vigorously. 100% ¹⁸O-water labeling results confirmed our hypothesis by showing complete labeling of the 1,5-InsP₈ pool within 30 min while 5-InsP₇ maintained a plateau between 60 and 70% (Figure S17). In contrast to the inositol pyrophosphates, InsP6 was labeled only very slowly, showing 12% ¹⁸O labeling after 60 min (Figure 5C). This suggests that the InsP₆ pool is relatively static regarding its synthesis from InsP₅, whereas the inositol pyrophosphates undergo a highly dynamic, permanent turnover of their phosphate groups. Since

both PP-InsPs are synthesized from InsP $_6$, turnover of their phosphate groups can be attributed almost exclusively to the exchange of the β -phosphates of their diphosphate groups. Remarkably, this high turnover occurs even under constant nutrient availability. It hence appears to be a constitutive feature of inositol pyrophosphate metabolism.

The analysis of lower phosphorylated InsPs using the same experimental approach revealed further interesting behavior. InsP₃, which is generated from PtdIns(4,5)P₂ through phospholipase C (Figure 1), incorporated ¹⁸O into ca. 50% of the pool within 1 min (Figure 5G,H). The InsP₃ pool could be dissected into two different species with similar dynamics. To assign the InsP₃ isomers, a homemade [¹³C₆] InsP₃ reference solution was generated by incubating [13C6] InsP6 (prepared with ultrapure water) at 100 °C for 5 h.50 The assignment of each generated [13C6] InsP3 isomer was achieved by a previously described method. To One of the ¹⁸O-InsP₃ species that we observed has the same electrophoretic migration time as Ins(1,4,5)P₃, Ins(1,3,4)P₃, and Ins(1,4,6)P₃ (Figure S18), which cannot be differentiated with our method. Considering published data, 18,51,52 we infer that its identity is most likely Ins(1,4,5)P3, the direct product of PtdIns(4,5)P₂ hydrolysis. The other labeled InsP₃ species does not comigrate with any reference InsP3 isomer that is available in our laboratory. Since the only InsP₃ reference for which this applies is Ins(2,4,6)P₃, we tentatively assign this species as Ins(2,4,6)P₃. Interestingly, the incorporation of up to five ¹⁸O labels into InsP3 was detected by CE-qTOF, suggesting that several phosphate groups undergo exchange. This is in stark contrast to what we observed for, e.g., InsP6 or InsP7. For Ins(1,4,5)P₃, this highly dynamic turnover may occur while it still forms the headgroup of PtdIns(4,5)P₂, but Ins(2,4,6)P₃

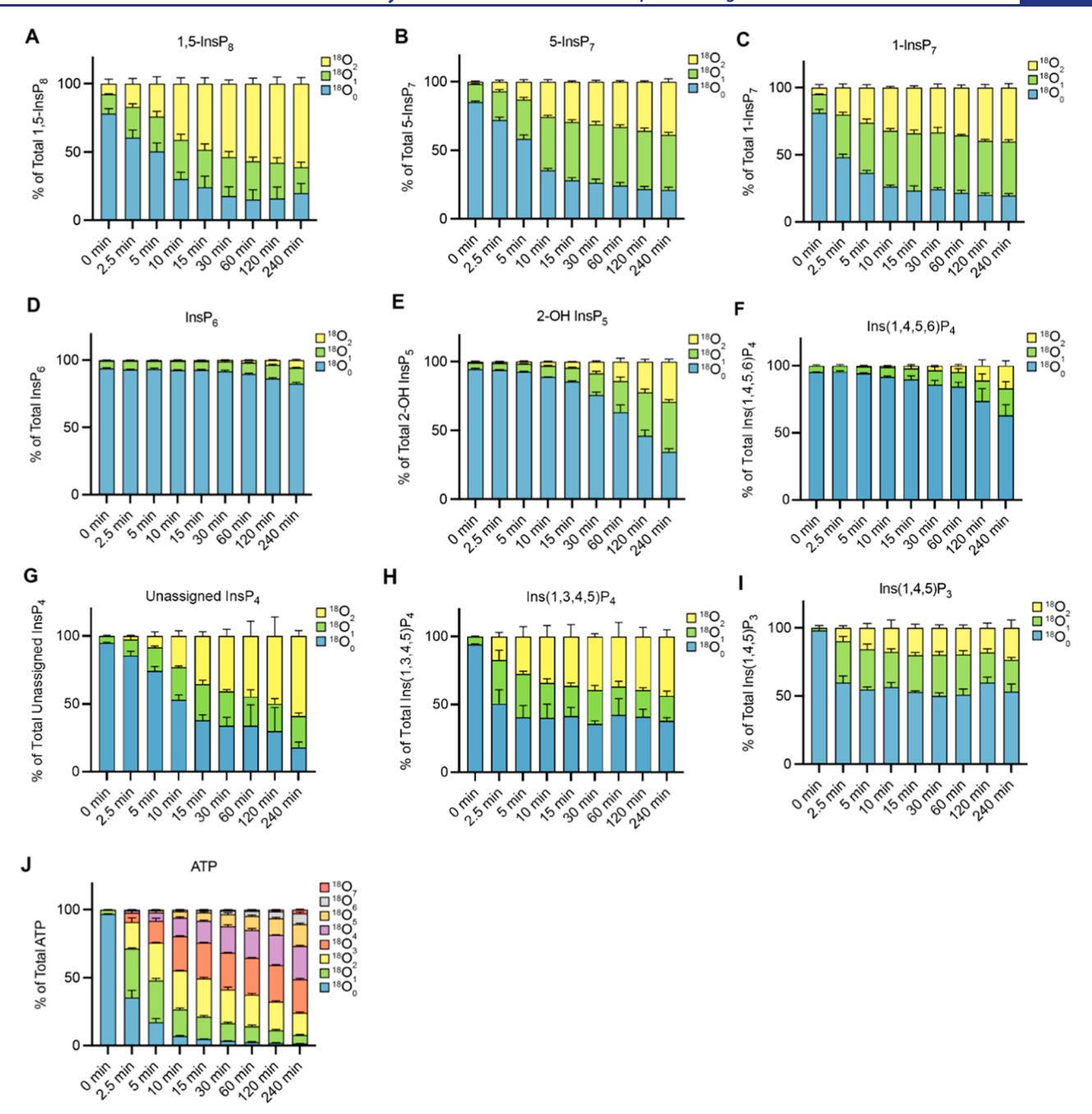


Figure 7. Kinetics of 18 O entry into ATP and cytosolic InsPs from human cells. Kinetics of 18 O entry into 1,5-InsP $_8$ (A), 5-InsP $_7$ (B), 1-InsP $_7$ (C), InsP $_6$ (D), 2-OH InsP $_5$ (E), Ins(1,4,5,6)P $_4$ (F), unassigned InsP $_4$ (G), Ins(1,3,4,5)P $_4$ (H), Ins(1,4,5)P $_3$: Ins(1,4,5)P $_3$: Ins(1,4,5)P $_3$: In, and ATP (J) were monitored in mammalian cells. HCT116 cells were grown in DMEM medium, detached, and collected by centrifugation. The cell pellet was resuspended in DMEM medium prepared with 50% of 18 O-labeled water. After the indicated periods of further incubation at 37 $^{\circ}$ C, aliquots of the cells were extracted with perchloric acid. CE-MS analyses of the extracts were performed and rare analytes (PP-InsPs) were measured in wide mass resolution. The means of three replicates are shown with standard deviations.

does not directly derive from this lipid⁵¹ and might undergo lipid-independent turnover (Figures 5I,J, and S19).

InsP₄ showed comparably limited turnover (Figure 5E,F) and could be dissected into two different InsP₄ species. One of them, assigned as Ins(1,3,4,5)P₄ (Figure S20), was static after 1 min and incorporated ¹⁸O to ca. 20%. The other one, which currently cannot be unambiguously assigned, showed very sluggish but continuous ¹⁸O incorporation. The different pools of InsP₄ very likely represent positional isomers with regard to the phosphate groups and not diastereomeric inositol core structures, such as *scyllo* inositol.

Combining the results with observations of the different dynamic phosphate exchanges among various InsPs in yeast, we propose a three-cycle model in which phosphate cycling occurs on discrete compounds along the inositol phosphate metabolic pathway (Figure 5K). For example, in the cycle of InsP₆ and inositol pyrophosphates (5-InsP₇; 1,5-InsP₈), highly dynamic phosphate conversion from InsP₆ to 5-InsP₇ was observed and 5-InsP₇ further interconverts with 1,5-InsP₈. In this cycle, only the β -phosphates are dynamic.

Inositol pyrophosphates are key regulators of P_i homeostasis. Their levels decrease under P_i starvation and inhibiting their

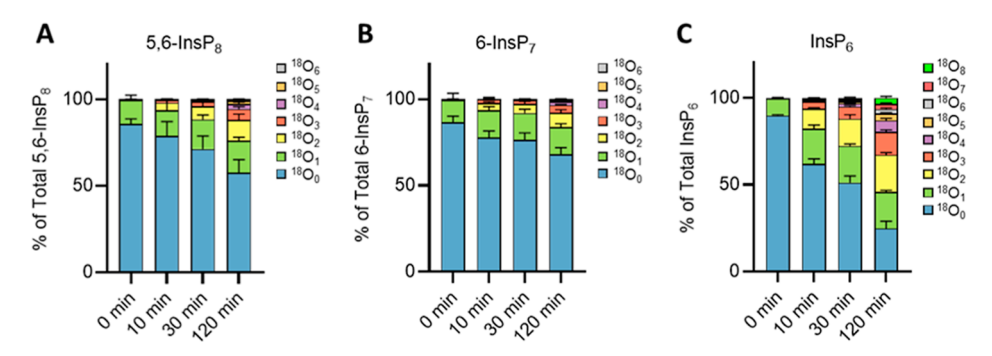


Figure 8. Kinetics of ¹⁸O entry into soluble InsPs from *D. discoideum*. Kinetics of ¹⁸O entry into 5,6-InsP₈ (A,) 6-InsP₇ (B), and InsP₆ (C) monitored in *Dictyostelium*. Cells were precultured in SIH medium and transferred to SIH media made of 50% of ¹⁸O-labeled water with P_i. After further incubation for the indicated periods of time, samples were harvested and extracted. Extracts were measured by CE-QQQ with wide mass resolution. The means of four replicates with standard deviations are shown.

synthesis induces a constitutive P_i starvation response. S3-56 The synthesis of these inositol pyrophosphates is regulated by intracellular P_i and by ATP levels, which is strongly correlated with P_i availability. We hence used ^{18}O labeling to investigate differences in inositol pyrophosphate turnover during P_i starvation. As shown in Figure 6A, both 5-Ins P_7 and 1-Ins P_7 exhibited lower ^{18}O incorporation under P_i -starved conditions as compared to those under P_i -rich conditions. This difference appeared as early as 1 min and became more pronounced over time. By contrast, Ins P_6 , which remains relatively stable during P_i starvation, showed little difference in ^{18}O labeling. These results illustrate the rapid and selective impact of P_i starvation on the turnover of higher inositol pyrophosphates on a minute time scale.

We also compared the 18 O labeling in a vip1 Δ mutant that fails to synthesize $InsP_8$ and 1- $InsP_7$ but accumulates more than 10-fold higher 5- $InsP_7$ levels. Under P_i -rich conditions, 18 O labeled 5- $InsP_7$ was accumulated to a greater extent in the vip1 Δ mutant compared to the wild type, particularly after 10 min (Figure 6B), whereas the ratio of 18 O labeled $InsP_6$ to unlabeled $InsP_6$ remained similar. 18 O incorporation into the ATP pool remained the same in both strains (wild type and vip1 Δ) (Figure 5).

2.3. Kinetic Compartmentalization of the InsP Pathway in Human Cells. Next, we tested the suitability of ¹⁸O-water to label inositol phosphates in HCT-116 cells. These experiments employ larger volumes of media and were hence performed with 50% ¹⁸O-water only to reduce the cost. Cells were pulse-labeled by transferring them into medium made with 50% ¹⁸O-water but of otherwise identical composition. At different time-points of pulse-labeling, aliquots were extracted with perchloric acid and analyzed by CE-MS (Figure 7).

¹⁸O rapidly entered ATP and the inositol pyrophosphates (5-InsP₇; 1-InsP₇; 1,5-InsP₈; data collected in wide mass resolution), reaching equilibrium after 10–20 min. Between 20 and 25% of these PP-InsPs remained unlabeled. InsP₆ labeling proceeded slowly also in mammalian cells, reaching only 1/6th of the pool after 4 h. This incorporation probably reflects new synthesis of InsP₆ through cell growth because the generation time of the cells under these steady media conditions is around 24 h. During the 4 h of labeling time, biomass would thus increase by roughly 1/6th, accounting for the increase in labeled InsP₆, which is of the same order. Interestingly, 2-OH InsP₅, which is of similar abundance as InsP₆ in some mammalian cells, ⁴⁵ showed significantly faster labeling than InsP₆, suggesting that the flux from InsP₅ to InsP₆ by the

inositol-pentakisphosphate 2-kinase (IPPK) is sluggish. The appearance of only two labels suggests that turnover takes place at a specific position and not at many different positions, as this would lead to higher numbers of ¹⁸O incorporations.

Each InsP₄ isomer showed different ¹⁸O incorporation patterns. Ins(1,4,5,6)P₄ (assignment shown in Figure S20), which is not observed in yeast, exhibited relatively slow incorporation of ¹⁸O, similar to InsP₆, whereas 80% of a currently unassigned InsP₄ was labeled to more than 80% with ¹⁸O over 4 h. This unassigned InsP₄ is different from the unassigned InsP₄ in yeast. Similarly as in yeast, Ins(1,3,4,5)P₄ incorporated ¹⁸O very rapidly, reaching a plateau within 2.5 min that remained constant for the rest of the 4 h incubation period.

We could also resolve three peaks of $InsP_3$. By comparison with ^{13}C -labeled internal references (Supplementary Figure S18), we assign the first one as $Ins(1,2,3)P_3$. The second peak remains ambiguous ($Ins(1,2,6)P_3$ and/or its enantiomer $Ins(2,3,4)P_3$). Both signals are apparently not significantly generated through kinases, which would lead to incorporation of the ^{18}O label. They might, however, originate from dephosphorylation of $InsP_6$ into these metabolites (see the Discussion). Since generation of $Ins(1,2,6)P_3$ through dephosphorylation by MINPP1 was recently described using ^{13}C NMR labeling, 15 the second peak thus likely represents $Ins(1,2,6)P_3$.

The third peak was assigned as $Ins(1,4,5)P_3$ as the most likely species. It incorporated ¹⁸O very rapidly and similarly as $Ins(1,3,4,5)P_4$ attained a plateau within 2.5 min that remained constant for the rest of the 4 h incubation. As in yeast, up to five ¹⁸O labels of $Ins(1,4,5)P_3$ were detectable by CE-qTOF within 15 min, suggesting turnover of multiple phosphate groups (Figure S21). Unfortunately, we could not record these multiple ¹⁸O labels accurately beyond 15 min because of matrix effects in these sample sets. Labeling did not reach the entire pool of $Ins(1,4,5)P_3$. Thus, similarly as argued above for yeast, there might be subpools of this compound, some of which remain quite static and others that turn over rapidly and are responsible for the initially rapid yet limited integration of ¹⁸O into the total pool of $Ins(1,4,5)P_3$.

Together, these data suggest massively different dynamics of phosphate exchange on InsPs also in mammalian cells: highly dynamic phosphate cycling of the P-anhydrides in the inositol pyrophosphate pools (5-InsP₇; 1-InsP₇; 1,5-InsP₈) and of phosphate esters in InsP₃ - likely resulting from the lipid-dependent turnover and cleavage by PLC—is separated by a

much more inert pool of InsP₆. 2OH-InsP₅ shows an intermediate behavior, and for InsP₄ turnover can be very rapid or sluggish, depending on the isomer. Thus, the inositol pyrophosphate and InsP₃ pools may cycle independently from each other, be connected through slower biosynthetic reactions, or be separated by compartmentalization.

2.4. ¹⁸O-Water Pulse Labeling Reveals a Sluggish PP-InsPs Metabolism in Amoeba. Finally, we performed similar labeling and extraction experiments with 50% ¹⁸O-water with the slime mold *Dictyostelium discoideum* (Figure 8). This organism has played an important role in the discovery of PP-InsPs as its concentrations are comparably high, reaching submillimolar levels. ⁵⁷ It produces a range of PP-InsP isomers different from those found, for example, in yeast and mammals. ^{14,58} In *D. discoideum*, around 75% of total ATP had incorporated ¹⁸O within 10 min of incubation (Figure S22). These proportions changed only a little in the subsequent 20 min, suggesting the existence of two pools of ATP that turn over at different velocities.

Labeling of InsP7 and InsP8 was much slower than in yeast and human cells: only 32% InsP7 and 44% InsP8 incorporated labels throughout the 2 h of incubation time. Considering the approximately 8 h generation time of Dictyostelium, the rate of incorporation into InsP7 may reflect new biosynthesis due to growth of the culture. The labeling of InsP8 goes beyond that but is far from the vigorous turnover observed in yeast and mammalian cells. InsP₆ labeling, on the other hand, proceeded much faster than that of the inositol pyrophosphates, and it was also more rapid and extensive than the labeling of InsP6 in yeast and human cells. Up to eight ¹⁸O labels were detected throughout the experiment, necessitating rapid phosphate group exchange at multiple positions in InsP₆. Thus, not only are the dynamics of InsPs metabolism in Dictyostelium significantly different than in budding yeast or mammalian cells but also the number of phosphate groups that undergo exchange. Unfortunately, the sensitivity needed to obtain a comprehensive analysis of the labeling of InsP₅, InsP₄, and InsP₃ was affected by the abundant and broad ethylenediaminetetraacetic acid (EDTA) signal present from the extraction buffer. For this reason, we do not report lower InsPs from these samples.

3. DISCUSSION

The metabolism of InsPs and PP-InsPs, which are signaling molecules of low abundance, has mainly been studied using radioactive labeling of inositol or of phosphate. 13,19 For inositol poly- and pyrophosphates, the labeling approach with ¹⁸O-water that we present here offers several important advantages, particularly for analyzing turnover of the phosphate groups. 34,37,59 18O is a stable, nonradioactive isotope, such that media and samples produced with it can be stored for extended periods of time. ¹⁸O-water can be obtained in a 99.5% pure form, enabling labeling to a very high specific isotope content. This facilitates detection of inositol phosphates by mass spectrometry, some of which exist in submicromolar concentrations in cells. 50,53,60,61 18O-water labeling can be performed in any medium and under any growth condition. This is a distinctive advantage over labeling with radioactive inositol. Cellular membranes are also permeable to water, which allows very rapid labeling (seconds, as compared to hours for inositol labeling) to high specific isotope content and apparent equilibrium. In combination with CE-MS detection, this facilitated the analysis of an

unexpectedly rapid turnover of phosphate groups around the inositol ring with high specificity. Turnover can be monitored simultaneously for a variety of InsPs in the same experiment.

The possibility of monitoring the kinetics of phosphate group turnover on InsPs with improved temporal resolution, sensitivity, throughput, and cost renders it possible to analyze flux through the metabolic pathways interconnecting inositol phosphates. Our method can detect inositol phosphates with high accuracy if applied in the unit-resolution or wideresolution mode for singly charged ions. For doubly charged anions, wide resolution produces a skewing from the true value that is on the order of 10% and unit mass resolution is preferable. However, under these conditions, the sensitivity of the wide mass resolution method is higher, which enables monitoring of metabolites and isotopologues of low abundance. The method also allows labeling of inositol phosphate lipids. We currently exploit this to derive metabolic network models for inositol polyphosphate metabolism and to explore the dynamics of inositol lipids, aspects that will be described in separate studies. One such network model for the inositol pyrophosphates has now become available.⁶²

Our analysis relies on the very high turnover of ATP inside cells, which renews and labels the entire ATP pool at the time scale of seconds to a few minutes, depending on the cell type. 42 Label can then be transferred to inositol phosphates by the respective kinases, and it can be removed again by hydrolysis through phosphatases. The efficiency of this ¹⁸O-water labeling approach is illustrated by the rapid labeling kinetics that we could uncover for some compounds in yeast, such as the PP-InsPs and some InsP₃ species (Figure 5K). Other pools of inositol phosphates, such as InsP₆ and InsP₄, incorporated ¹⁸O very slowly, suggesting at first sight a very low turnover. It is worthwhile to consider the enzymatic aspect of this process. Kinases transfer phosphate from ATP through a variety of mechanisms.⁶³ A common feature is that the γ -phosphate of ATP undergoes an attack, for example, by an OH group of the substrate to be phosphorylated. When ADP leaves, the oxygen constituting the link to the phosphorylated substrate stems from the unlabeled substrate, not from the $^{18}\mathrm{O}$ labeled γ phosphate group. If the substrate is dephosphorylated again, labeled water attacks the phosphate group and the substrate leaves, keeping its unlabeled oxygen. 64 Label is thus introduced by the kinase reaction and withdrawn by the opposing phosphatase reaction. We may then expect that the substrate is ¹⁸O labeled only as long as it maintains the labeled phosphate group. Therefore, InsP6 should not be considered a truly static pool. The rapid labeling of 5-InsP7 through InsP6 kinase requires cycling of the β -phosphate on position 5 of the inositol ring and engages InsP6 as a substrate. Thus, there should be rapid cycling between InsP₆ and 5-InsP₇ by phosphorylation and dephosphorylation, but it does not leave a corresponding ¹⁸O mark on InsP₆. Along the same lines, we expect the labeling of 2OH-InsP5 to stem from the phosphorylation of InsP₄ through inositol polyphosphate multikinase. That this accumulating label is propagated only very inefficiently from 2OH-InsP₅ into InsP₆ argues for a sluggish exchange between InsP5 and InsP6 under the conditions we investigated. For similar reasons, we expect the interconversion of $InsP_3$ and $InsP_4$ to be slow (Figure 5K).

These very pronounced differences in turnover suggest that phosphate cycling can occur on discrete compounds along the inositol phosphate metabolic pathway. This can separate the rapidly interconverting InsP₇ and InsP₈ from sluggish

interconversions between $InsP_3$ and $InsP_4$ and between $InsP_5$ and $InsP_6$ (Figure 5K). It suggests that even though $InsP_4$ through $InsP_8$ derive from $InsP_3$ and enzymes can interconvert all these compounds (Figure 1), 18,52,65 they do not operate as a simple linear pathway. Instead, InsPs appear to be organized into a series of separated phosphate cycles. In this way, each cycle is free to mediate independent signaling processes. The metabolic reactions connecting the cycles may then serve mainly to replenish or diminish substrate levels in the cycle, for example, when growth or changing nutrient conditions may necessitate an adaptation of the signaling properties. Such a scenario arises, for example, upon phosphate replenishment after starvation, when the $InsP_7$ and $InsP_8$ pools become significantly expanded. $^{6,53-55}$

Turnover of PP-InsPs and InsP₃ is very vigorous, even under steady growth conditions, i.e., under constant nutrient supply and growth. Such strong turnover implies permanent competing synthesis and degradation of the compounds. The simultaneous activity of two antagonizing reactions is often considered as "wasteful cycling". It may, however, be worth the price because it comes with significant benefits and additional potential for information transmission. Substrate cycling can sharpen the responses of a signaling system and increase its sensitivity. It can amplify signals, ^{66,67} allow to filter or process information from noise in external and internal parameters, and create bistable switches. 68,69 This makes, for example, the rapid cycling of 1,5-InsP₈ interesting and potentially relevant because the yeast PHO pathway is controlled by 1,5-InsP₈, exploits expression noise, and behaves like a bistable switch.⁷⁰⁻

Some inositol phosphates, such as 5-InsP₇ in yeast or InsP₃ in human cells, showed biphasic labeling kinetics, where a rapid initial turnover was followed by a long phase in which no or only negligible further ¹⁸O was incorporated. Since the cells had been growing under steady conditions, it is unlikely that this reflects a sudden change in the metabolism of these compounds. A more plausible explanation is sequestration of the compound into pools of greater or lesser accessibility to metabolizing enzymes. Such sequestration can be realized by stable binding of InsPs to proteins⁷⁴ or other molecules and/or by transfer into distinct subcellular compartments. For InsPs, several examples show that they can integrate into proteins in an apparently very stable fashion such that the interaction persists even through purification and crystallization of the proteins. Examples include the capsid and Gag proteins of retroviruses, ^{75–77} the RNA editing enzyme ADAR2, or casein kinase 2. ^{78,79} Moreover, InsPs might be sequestered into biomolecular condensate type structures such as nucleoli.80 Such mechanisms may also localize InsPs to cytosolic areas with greater or lesser availability of labeled ATP because the distribution of ATP in the cytosol is inhomogeneous.^{81–83}

Another, equally interesting possibility is that subpools of the same compound show different turnover rates because they reflect heterogeneities in the cell population. Cell populations, even those of simple unicellular organisms, are heterogeneous. The cells are in different metabolic, signaling, and cell cycle states, which can sometimes be quite stably maintained to ensure diversity in the population. Hen, different cell states may give rise to differences in InsP turnover, which we revealed here. Some InsPs undergo indeed significant changes during the cell cycle. Investigating such heterogeneities systematically becomes accessible with our approach since it is nonradioactive and sensitive, thus allowing to sort cell

populations into specific subpools, for example, by fluorescence-activated cell sorting, to dissect the diversity in their InsPs metabolism.

In addition to analyzing the turnover of individual InsPs using the ¹⁸O labeling method, the approach can also be applied to understand how InsPs dynamics change under different physiological conditions, such as those shown for Pirich vs P_i-depleted conditions (Figure 6A) or in KO cell lines, such as $vip1\Delta$ (Figure 6B). For example, we observe an increased turnover of inositol pyrophosphates under phosphate-rich conditions as compared with phosphate-depleted conditions, while InsP₆ and ATP turnover remain unchanged. Rapid pulse labeling by ¹⁸O-water followed by CE-MS allows to generate kinetic data of significantly better time and isomer resolution than the traditional radioactive approaches. 13 Combining this approach with controlled changes in growth conditions or the acute stimulation or inhibition of signaling pathways should allow us to obtain novel insights into the regulation and signaling properties of inositol phosphate pools. It will help us to create metabolic models of inositol phosphate-based signaling pathways and to better understand effects exerted by kinase inhibitors on cellular inositol phosphate fluxes, an area of growing interest in, for example, metabolic diseases.⁸⁶ Indeed, the data sets obtained herein have already served as the basis to create mathematical models of the inositol pyrophosphate network.⁶²

In striking contrast to the situation in yeast and human cells, we observed a sluggish PP-InsP turnover but unexpectedly high turnover of ${\rm InsP_6}$ occurring on many of its different phosphate groups in the amoeba D. discoideum. Its lethargic PP-InsP turnover suggests that the amoeba employs these metabolites differently than yeast or mammalian cells. This correlates with the diversification of the InsP-kinase families that are used in different eukaryotic clades to drive InsPs metabolism and signaling 87 and with the complexity of the enzymology of PP-InsPs metabolism in amoeba, which is far greater than in yeast or mammalian cells. 58 The strikingly different behavior of Dictyostelium calls for a detailed analysis of InsP fluxes, which may uncover new strategies for InsP signaling. The methods presented here open the door to such investigations.

4. MATERIAL AND METHODS

4.1. Cell Strains and Culture Media. 4.1.1. Yeast. The Saccharomyces cerevisiae strain BY4741 (MATa his $3\Delta 1$ leu $2\Delta 0$ met $15\Delta 0$ ura $3\Delta 0$) was used in this study. The vtc 4Δ and vip 1Δ mutant strains were used as in the previous studies, ref 88 and ref 53, respectively. Yeast cells were shaken (150 rpm, 30 °C, unless stated otherwise) in SC medium: 6.7 g/L yeast nitrogen base (Formedium, USA) and 2% of glucose.

Medium for $^{18}\mbox{O}$ labeling was prepared as a 2× concentrated SC stock made with normal water in advance, which was then diluted by an equal volume of 99% $^{18}\mbox{O}$ -water (Medical Isotopes Inc.) to make SC with 50% $^{18}\mbox{O}$ -water. The P_i -free medium was prepared using yeast nitrogen base without phosphate (Formedium, USA).

4.1.2. Mammalian Cells. HCT116^{UCL} cells were used in this study. Cells were grown for 6 passages in DMEM-HAM's F12 (Gibco) supplemented with 10% (v/v) fetal calf serum, 50 U/ml penicillin, 50 mg/mL streptomycin, 5 μ g/mL insulin. Cells were grown at 37 °C in 5% CO₂ with 98% humidity.

5% $\rm CO_2$ with 98% humidity. For $^{18}\rm O$ labeling, a 2× concentrated medium was prepared using DMEM powder (Sigma) supplemented with 7.4 g/L sodium bicarbonate. This stock was diluted by an equal volume of $^{18}\rm O$ -labeled water to yield the medium with 50% $^{18}\rm O$ -water that was used for the experiments.

- 4.1.3. Dictyostelium. D. discoideum strain AX2 obtained from dictyBase (http://dictybase.org) was used in this study. Amoeba were grown at 22 °C with gentle shaking (100 rpm) in synthetic SIH medium (Formedium, #SIH0101). Medium for ¹⁸O labeling was prepared as a 2× concentrated SIH stock made with ddH2O, which was then diluted by an equal volume of 99% ¹⁸O-water (Medical Isotopes Inc.) to make SIH with 50% ¹⁸O-water.
- 4.2. Extraction of InsPs and ATP. 4.2.1. Yeast. Yeast cells were grown at 20 °C overnight in 50 mL of SC medium to reach logarithmic phase $(4.3 \times 10^7 \text{ cells/ml})$ in the morning. 4 ml samples were harvested by centrifugation (3200g, 3 min, 20 °C) and resuspended in the same volume of SC prepared with 50% of ¹⁸Olabeled water. Cells were further incubated under the same

3 ml of yeast culture $(4.3 \times 10^7 \text{ cells/ml})$ was mixed with 300 μ L of 11 M perchloric acid to a final concentration of 1 M. Samples were snap-frozen in liquid nitrogen and then centrifuged at 20,000g for 3 min at 4 °C. The soluble supernatant was transferred to a new tube, and each sample was supplemented with 6 mg of titanium dioxide (TiO₂) beads (GL Sciences, Japan), which had been prerinsed through two rounds of washing with 1 mL of H₂O and 1 M perchloric acid, respectively. The mixture was gently rotated for 15 min at 4 °C and centrifuged at 20,000g for 3 min at 4 °C. The TiO2 beads were washed twice using 500 µL of 1 M perchloric acid. InsPs and ATP were eluted by incubating the beads with 300 μ L of 3% (v/v) NH₄OH for 5 min at room temperature under gentle shaking. After centrifugation at 20,000g for 3 min, the eluents were transferred to a new tube. Any remaining TiO₂ beads were removed by centrifugation at 20,000g for 3 min. The resulting supernatant was completely dried in a SpeedVac (Labogene, Denmark) at 42 °C. Samples were kept at −20 °C until analysis.

For experiments under P_i-rich and P_i-starvation conditions, yeast cells were first grown in a Pi-rich medium at 20 °C overnight. Upon reaching the logarithmic phase, the culture was split into two and washed twice with either a P_i-rich or P_i-free medium prepared with normal water. Cells were then resuspended in an ¹⁸O-labeled P_i-rich or ¹⁸O-labeled P_i-free medium. Samples were harvested at different time points using the same procedure and InsPs were extracted as described above.

4.2.2. Human Cells. HCT116^{UCL} cells were seeded in 10 cm² Petri dishes and grown to 80% confluence (6.5 \times 10⁶ cells) at 37 °C as described above. Cells were detached from the Petri dish by adding 5 mL of 0.25% Trypsin (Thermo Fisher Scientific, USA) and harvested by centrifugation at 3200g for 5 min. The cell pellet was resuspended in 1 mL of DMEM medium (Thermo Fisher Scientific, USA) prepared with 50% of ¹⁸O-labeled water and further incubated at 37 °C.

At different time points, 1 mL of samples were mixed with 100 μ L of 11 M perchloric acid. After snap-freezing in liquid nitrogen, samples were centrifuged at 16,000g in a tabletop centrifuge. The soluble supernatant was transferred into a new tube and mixed with prewashed TiO₂ beads (5 mg of beads per sample). The extraction was performed in the same way as for yeast.

- 4.2.3. D. discoideum. D. discoideum cells were seeded at $2-5 \times 10^5$ cells/ml and grown for 24-48 h in 50 mL of SIH medium to reach a cell density of $1-3 \times 10^6$. Amoeba (8 × 10⁶ per experimental point) were transferred into a 15 mL falcon tube, harvested by centrifugation (800g, 5 min, 22 °C), and resuspended in 2 mL of SIH medium prepared with 50% of ¹⁸O-water. Cells were further incubated under the same conditions. At specific time points, the falcon tube was spun (1000g, 2 min, 4 °C) and the cell pellet snap-frozen in liquid nitrogen. At the end of the experiment, each cell pellet was resuspended in 1 M perchloric acid with 5 mM EDTA and InsPs subjected to TiO₂
- purification as previously described. 47,48 **4.3. Potential** 16/18 Oxygen Exchange. 4.3.1. ATP in the Presence of 18O-Water or Inositol Hexakisphosphate Kinase IP6K1. After incubating 1 mM of ATP with ¹⁶O-water, 50% of ¹⁸Owater (>98 atom % 18O), IP6K1 reaction buffer (50 mM NaCl, 20 mM HEPES, 6 mm MgCl₂, 1 mM DTT, pH 6.8), and purified IP6K1

- $(0.0375 \,\mu\mathrm{g}/\mu\mathrm{L})^{89}$ at 37 °C for 4 h, samples were diluted 2-fold and measured by CE-QQQ with unit mass resolution.
- 4.3.2. InsPs and PP-InsPs in the Presence of ¹⁸O-Water. After incubating 4 μM of Ins(1,4,5)P3, Ins(1,3,4,5)P4, 2-OH InsP5, InsP6, 5-InsP7, and 1,5-InsP8 with 50% of ^{18}O -water (>98 atom % ^{18}O) at 37 °C for 4 h, samples were measured by CE-QQQ with unit mass
- 4.3.3. InsPs and PP-InsPs in the Presence of Inositol Hexakisphosphate Kinase IP6K1. After incubating 100 µM of InsP₆ or 5-InsP₇ with 50% ¹⁸O-water (>98 atom % ¹⁸O), IP6K1 reaction buffer (50~mM NaCl, 20 mM HEPES, 6 mm MgCl₂, 1 mM DTT, pH 6.8), and purified IP6K1 (0.0375 $\mu g/\mu L$) at 37 °C for 4 h, samples were diluted 2-fold and measured by CE-QQQ with unit mass resolution.
- 4.3.4. Extraction of InsPs and PP-InsPs in the Presence of ¹⁸O-Water. 4 µM of InsP₆, 5-InsP₇, 1-InsP₇, and 1,5-InsP₈ were added to 800 μ L of 1 M perchloric acid containing 50% (v/v) of ¹⁸O-water and InsPs subjected to TiO₂ purification as described above. Samples were then measured by CE-QQQ with a unit mass resolution.
- 4.3.5. IP6K1 In Vitro Assay. 100 μM InsP₆ was incubated with 1 mM ATP or $^{18}O_2$ ATP, IP6K1 reaction buffer (50 mM NaCl, 20 mM HEPES, 6 mm MgCl₂, 1 mM DTT, pH 6.8), and purified IP6K1 $(0.0375 \mu g/\mu L)$ in the presence of 50% (v/v) of ¹⁸O-water or 100% of ¹⁶O-water at 37 °C for 4 h. Then, samples were placed on ice, and the enzymatic activity was quenched by adding $10~\mu\mathrm{M}$ (working concentration) EDTA. After 2-fold dilution, samples were measured by CE-QQQ with unit mass resolution.
- 4.4. CE-ESI-MS Analysis of InsPs, PP-InsPs, and ATP. 4.4.1. CE-qTOF. An Agilent 7100 capillary electrophoresis system coupled to a qTOF (Agilent 6520) equipped with a commercial CE-MS adapter and sprayer kit (from Agilent) was used. The sheath liquid (water: isopropanol = 1:1, v/v) spiked with mass references $(TFA anion, [M - H]^-, 112.9855; HP-0921, [M - H +$ CH₃COOH]⁻, 980.0163) was introduced with a constant flow of 6 μ L/min. A bare fused silica capillary with a length of 100 cm (50 μ m internal diameter and 365 μ m outer diameter) was used for CE separation. The background electrolyte (35 mM ammonium acetate titrated with ammonium hydroxide to pH 9.75) was employed for all of the experiments. Before the run, the capillary was flushed with background electrolytes for 400 s. 30 or 40 nL of sample was injected by applying pressure (100 mbar for 15 or 20 s). The qTOF was conducted in negative ionization mode. MS source and scan parameters shown in Table S1. Biological samples were analyzed by Acquisition mode MS1. For the ESI-MS fragmentations of ATP and 5-InsP₇, Acquisition mode Auto MS2 was employed.
- 4.4.2. CE-QQQ. We used an Agilent 7100 capillary electrophoresis system coupled to an Agilent 6495C Triple Quadrupole system, adopting an Agilent CE-MS interface. The sheath liquid (water/ isopropanol = 1:1, v/v) was introduced with a constant flow of 10 μ L/min. A bare fused silica capillary with a length of 100 cm (50 μ m internal diameter and 365 μm outer diameter) was used for CE separation. The background electrolytes (35 mM ammonium acetate titrated with ammonium hydroxide to pH 9.75) was employed for all experiments. Before running the samples, the capillary was flushed with background electrolytes for 400 s. 30 nL of sample was injected by applying pressure (100 mbar for 15 s). Negative ionization mode was employed. MS source parameters are shown in Table S2. For yeast and HCT116 cell samples, MRM transition settings are shown in Tables S3, S4, and S5. For amoeba samples, MRM transition settings are shown in Tables S3, S6, S7, and S8. All samples are measured by CE-QQQ unless specifically stated otherwise.

ASSOCIATED CONTENT

Supporting Information

The Supporting Information is available free of charge at https://pubs.acs.org/doi/10.1021/jacs.4c16206.

Instrument and scan source parameters, MRM transitions settings of ATP and InsPs, oxygen migration (scrambling) on ATP and 5-InsP₇ studies in the gas phase, extracted ion electropherograms of ATP and InsPs, spontaneous ^{16/18} oxygen exchange studies, ¹⁸O labeling pattern of ATP and 5-InsP₇ by CE-QQQ unit and wide resolution method, InsP₈ and InsP₇ labeling under 100% of ¹⁸O-labeled water, assignment of InsP₃ and InsP₄ isomers in yeast and HCT116 cells, qTOF analysis of InsP₃ in yeast and HCT116 cells, kinetics of ¹⁸O labeling entry into ATP in *D. discoideum*, and additional references (PDF)

AUTHOR INFORMATION

Corresponding Authors

Andreas Mayer — Département d'immunobiologie, Université de Lausanne, CH-1066 Epalinges, Switzerland; o orcid.org/0000-0001-6131-313X; Email: Andreas.Mayer@unil.ch

Henning Jacob Jessen — Institute of Organic Chemistry, University of Freiburg, 79104 Freiburg, Germany; CIBSS— Centre for Integrative Biological Signaling Studies, University of Freiburg, 79104 Freiburg, Germany; orcid.org/0000-0002-1025-9484; Email: henning.jessen@oc.unifreiburg.de

Authors

Geun-Don Kim — Département d'immunobiologie, Université de Lausanne, CH-1066 Epalinges, Switzerland; ⊙ orcid.org/0000-0002-3580-2471

Guizhen Liu — Institute of Organic Chemistry, University of Freiburg, 79104 Freiburg, Germany; CIBSS—Centre for Integrative Biological Signaling Studies, University of Freiburg, 79104 Freiburg, Germany

Danye Qiu – Institute of Organic Chemistry, University of Freiburg, 79104 Freiburg, Germany

Maria Giovanna De Leo – Département d'immunobiologie, Université de Lausanne, CH-1066 Epalinges, Switzerland

Navin Gopaldass – Département d'immunobiologie, Université de Lausanne, CH-1066 Epalinges, Switzerland

Jacques Hermes – CIBSS—Centre for Integrative Biological Signaling Studies and Institute of Physics, University of Freiburg, 79104 Freiburg, Germany

Jens Timmer – CIBSS—Centre for Integrative Biological Signaling Studies and Institute of Physics, University of Freiburg, 79104 Freiburg, Germany

Adolfo Saiardi — Medical Research Council, Laboratory for Molecular Cell Biology, University College London, WC1E 6BT London, U.K.; o orcid.org/0000-0002-4351-0081

Complete contact information is available at: https://pubs.acs.org/10.1021/jacs.4c16206

Author Contributions

*G.-D.K. and G.L. contributed equally to this work.

The authors declare no competing financial interest.

ACKNOWLEDGMENTS

This study was supported by the Deutsche Forschungsgemeinschaft (DFG) under Germany's excellence strategy (CIBSS, EXC-2189, Project ID 390939984, to H.J.J.). This project has received funding from the European Research Council (ERC) under the European Union's Horizon 2020 research and innovation program (grant agreement no. 864246, to H.J.J.). H.J. acknowledges funding from the Volkswagen Foundation (VW Momentum Grant 98604). This work was supported by grants from the SNSF (320030-

228119, 31003A_179306, and 310030_204713) and ERC (788442) to A.M. and by the HFSP (LT000588/2019) to G.-D.K. A.S. gratefully acknowledges the support of the UKRI Medical Research Council grant MR/T028904/1.

REFERENCES

- (1) Posor, Y.; Jang, W.; Haucke, V. Phosphoinositides as Membrane Organizers. *Nat. Rev. Mol. Cell Biol.* **2022**, 23 (12), 797–816.
- (2) Falkenburger, B. H.; Jensen, J. B.; Dickson, E. J.; Suh, B.; Hille, B. SYMPOSIUM REVIEW: Phosphoinositides: Lipid Regulators of Membrane Proteins. *J. Physiol.* **2010**, *588* (17), 3179–3185.
- (3) Monserrate, J. P.; York, J. D. Inositol Phosphate Synthesis and the Nuclear Processes They Affect. *Curr. Opin. Cell Biol.* **2010**, 22 (3), 365–373.
- (4) Shears, S. B.; Ganapathi, S. B.; Gokhale, N. A.; Schenk, T. M. H.; Wang, H.; Weaver, J. D.; Zaremba, A.; Zhou, Y. Phosphoinositides II: The Diverse Biological Functions. *Subcell. Biochem.* **2012**, *59*, 389–412.
- (5) Maffucci, T.; Falasca, M. Signalling Properties of Inositol Polyphosphates. *Molecules* **2020**, *25* (22), 5281.
- (6) Li, X.; Gu, C.; Hostachy, S.; Sahu, S.; Wittwer, C.; Jessen, H. J.; Fiedler, D.; Wang, H.; Shears, S. B. Control of XPR1-Dependent Cellular Phosphate Efflux by InsP8 Is an Exemplar for Functionally-Exclusive Inositol Pyrophosphate Signaling. *Proc. Natl. Acad. Sci. U.S.A.* 2020, 117, 3568–3574.
- (7) Moritoh, Y.; Abe, S.-I.; Akiyama, H.; Kobayashi, A.; Koyama, R.; Hara, R.; Kasai, S.; Watanabe, M. The Enzymatic Activity of Inositol Hexakisphosphate Kinase Controls Circulating Phosphate in Mammals. *Nat. Commun.* **2021**, *12* (1), 4847–4915.
- (8) Wild, R.; Gerasimaite, R.; Jung, J.-Y.; Truffault, V.; Pavlovic, I.; Schmidt, A.; Saiardi, A.; Jessen, H. J.; Poirier, Y.; Hothorn, M.; Mayer, A. Control of Eukaryotic Phosphate Homeostasis by Inositol Polyphosphate Sensor Domains. *Science* **2016**, 352 (6288), 986–990.
- (9) Szijgyarto, Z.; Garedew, A.; Azevedo, C.; Saiardi, A. Influence of Inositol Pyrophosphates on Cellular Energy Dynamics. *Science* **2011**, 334 (6057), 802–805.
- (10) Gu, C.; Liu, J.; Liu, X.; Zhang, H.; Luo, J.; Wang, H.; Locasale, J. W.; Shears, S. B. Metabolic Supervision by PPIP5K, an Inositol Pyrophosphate Kinase/Phosphatase, Controls Proliferation of the HCT116 Tumor Cell Line. *Proc. Natl. Acad. Sci. U.S.A.* **2021**, *118* (10), No. e2020187118.
- (11) Austin, S.; Mayer, A. Phosphate Homeostasis A Vital Metabolic Equilibrium Maintained Through the INPHORS Signaling Pathway. *Front. Microbiol.* **2020**, *11*, 1367.
- (12) Kim, S.; Bhandari, R.; Brearley, C. A.; Saiardi, A. The Inositol Phosphate Signalling Network in Physiology and Disease. *Trends Biochem. Sci.* **2024**, 49 (11), 969–985.
- (13) Wilson, M. S. C.; Saiardi, A. Importance of Radioactive Labelling to Elucidate Inositol Polyphosphate Signalling. *Top. Curr. Chem.* **2017**, 375 (1), 14.
- (14) Qiu, D.; Wilson, M. S.; Eisenbeis, V. B.; Harmel, R. K.; Riemer, E.; Haas, T. M.; Wittwer, C.; Jork, N.; Gu, C.; Shears, S. B.; Schaaf, G.; Kammerer, B.; Fiedler, D.; Saiardi, A.; Jessen, H. J. Analysis of Inositol Phosphate Metabolism by Capillary Electrophoresis Electrospray Ionization Mass Spectrometry. *Nat. Commun.* **2020**, *11* (1), 6035.
- (15) Trung, M. N.; Kieninger, S.; Fandi, Z.; Qiu, D.; Liu, G.; Mehendale, N. K.; Saiardi, A.; Jessen, H.; Keller, B.; Fiedler, D. Stable Isotopomers of Myo-Inositol Uncover a Complex MINPP1-Dependent Inositol Phosphate Network. *ACS Cent. Sci.* **2022**, 8 (12), 1683–1694.
- (16) Eisenbeis, V. B.; Qiu, D.; Gorka, O.; Strotmann, L.; Liu, G.; Prucker, I.; Su, X. B.; Wilson, M. S. C.; Ritter, K.; Loenarz, C.; Groß, O.; Saiardi, A.; Jessen, H. J. β -Lapachone Regulates Mammalian Inositol Pyrophosphate Levels in an NQO1- and Oxygen-Dependent Manner. *Proc. Natl. Acad. Sci. U.S.A.* **2023**, *120* (34), No. e2306868120.

- (17) Liu, G.; Riemer, E.; Schneider, R.; Cabuzu, D.; Bonny, O.; Wagner, C. A.; Qiu, D.; Saiardi, A.; Strauss, A.; Lahaye, T.; Schaaf, G.; Knoll, T.; Jessen, J. P.; Jessen, H. J. The Phytase RipBL1 Enables the Assignment of a Specific Inositol Phosphate Isomer as a Structural Component of Human Kidney Stones. *RSC Chem. Biol.* **2023**, *4* (4), 300–309.
- (18) Desfougères, Y.; Wilson, M. S. C.; Laha, D.; Miller, G. J.; Saiardi, A. ITPK1Mediates the Lipid-Independent Synthesis of Inositol Phosphates Controlled by Metabolism. *Proc. Natl. Acad. Sci. U.S.A.* **2019**, *116*, 24551.
- (19) Whitfield, H.; Riley, A. M.; Diogenous, S.; Godage, H. Y.; Potter, B. V. L.; Brearley, C. A. Simple Synthesis of 32P-Labelled Inositol Hexakisphosphates for Study of Phosphate Transformations. *Plant Soil* **2018**, 427 (1–2), 149–161.
- (20) Berridge, M. J.; Irvine, R. F. Inositol Trisphosphate, a Novel Second Messenger in Cellular Signal Transduction. *Nature* **1984**, 312 (5992), 315–321.
- (21) Brearley, C. A.; Hanke, D. E. Pathway of Synthesis of 3,4- and 4,5-Phosphorylated Phosphatidylinositols in the Duckweed Spirodela Polyrhiza L. *Biochem. J.* 1993, 290 (1), 145–150.
- (22) Brearley, C. A.; Hanke, D. E. Metabolic Evidence for the Order of Addition of Individual Phosphate Esters in the Myo -Inositol Moiety of Inositol Hexakisphosphate in the Duckweed Spirodela Polyrhiza L. *Biochem. J.* **1996**, 314 (1), 227–233.
- (23) Brearley, C. A.; Hanke, D. E. Inositol Phosphates in the Duckweed Spirodela Polyrhiza L. *Biochem. J.* **1996**, 314 (1), 215–225.
- (24) Auesukaree, C.; Homma, T.; Tochio, H.; Shirakawa, M.; Kaneko, Y.; Harashima, S. Intracellular Phosphate Serves as a Signal for the Regulation of the PHO Pathway in Saccharomyces Cerevisiae. *J. Biol. Chem.* **2004**, 279 (17), 17289–17294.
- (25) Nemutlu, E.; Juranic, N.; Zhang, S.; Ward, L. E.; Dutta, T.; Nair, K. S.; Terzic, A.; Macura, S.; Dzeja, P. P. Electron Spray Ionization Mass Spectrometry and 2D 31P NMR for Monitoring 18O/16O Isotope Exchange and Turnover Rates of Metabolic Oligophosphates. *Anal. Bioanal. Chem.* **2012**, 403 (3), 697–706.
- (26) Kotte, O.; Zaugg, J. B.; Heinemann, M. Bacterial Adaptation through Distributed Sensing of Metabolic Fluxes. *Mol. Syst. Biol.* **2010**, *6* (1), 355.
- (27) Kochanowski, K.; Volkmer, B.; Gerosa, L.; van Rijsewijk, B. R. H.; Schmidt, A.; Heinemann, M. Functioning of a Metabolic Flux Sensor in Escherichia Coli. *Proc. Natl. Acad. Sci. U.S.A.* **2013**, *110* (3), 1130–1135.
- (28) Nemutlu, E.; Gupta, A.; Zhang, S.; Viqar, M.; Holmuhamedov, E.; Terzic, A.; Jahangir, A.; Dzeja, P. Decline of Phosphotransfer and Substrate Supply Metabolic Circuits Hinders ATP Cycling in Aging Myocardium. *PLoS One* **2015**, *10* (9), No. e0136556.
- (29) Monge, M. E.; Dodds, J. N.; Baker, E. S.; Edison, A. S.; Fernández, F. M. Challenges in Identifying the Dark Molecules of Life. *Annu. Rev. Anal. Chem.* **2019**, *12* (1), 177–199.
- (30) Dawis, S. M.; Walseth, T. F.; Deeg, M. A.; Heyman, R. A.; Graeff, R. M.; Goldberg, N. D. Adenosine Triphosphate Utilization Rates and Metabolic Pool Sizes in Intact Cells Measured by Transfer of 18O from Water. *Biophys. J.* **1989**, 55 (1), 79–99.
- (31) Menniti, F. S.; Miller, R. N.; Putney, J. W.; Shears, S. B. Turnover of Inositol Polyphosphate Pyrophosphates in Pancreatoma Cells. J. Biol. Chem. 1993, 268 (6), 3850–3856.
- (32) Joshi, S. R.; Li, X.; Jaisi, D. P. Transformation of Phosphorus Pools in an Agricultural Soil: An Application of Oxygen-18 Labeling in Phosphate. *Soil Sci. Soc. Am. J.* **2016**, *80* (1), 69–78.
- (33) Wang, L.; Amelung, W.; Willbold, S. 18O Isotope Labeling Combined with 31P Nuclear Magnetic Resonance Spectroscopy for Accurate Quantification of Hydrolyzable Phosphorus Species in Environmental Samples. *Anal. Chem.* **2021**, 93 (4), 2018–2025.
- (34) Barneda, D.; Janardan, V.; Niewczas, I.; Collins, D. M.; Cosulich, S.; Clark, J.; Stephens, L. R.; Hawkins, P. T. Acyl Chain Selection Couples the Consumption and Synthesis of Phosphoinositides. *EMBO J.* **2022**, *41* (18), No. e110038.
- (35) Siegenthaler, M. B.; McLaren, T. I.; Frossard, E.; Tamburini, F. Dual Isotopic (33P and 18O) Tracing and Solution 31P NMR

- Spectroscopy to Reveal Organic Phosphorus Synthesis in Organic Soil Horizons. Soil Biol. Biochem. 2024, 197, 109519.
- (36) Hackney, D. D. Theoretical Analysis of Distribution of [180]Pi Species during Exchange with Water. Application to Exchanges Catalyzed by Yeast Inorganic Pyrophosphatase. *J. Biol. Chem.* **1980**, 255 (11), 5320–5328.
- (37) Versaw, W. K.; Metzenberg, R. L. Intracellular Phosphate–Water Oxygen Exchange Measured by Mass Spectrometry. *Anal. Biochem.* **1996**, 241 (1), 14–17.
- (38) Juranić, N.; Nemutlu, E.; Zhang, S.; Dzeja, P.; Terzic, A.; Macura, S. 31P NMR Correlation Maps of 18O/16O Chemical Shift Isotopic Effects for Phosphometabolite Labeling Studies. *J. Biomol. NMR* **2011**, *50* (3), 237–245.
- (39) Walker, J. E. ATP Synthesis by Rotary Catalysis (Nobel Lecture). Angew. Chem., Int. Ed. 1998, 37 (17), 2308-2319.
- (40) Müller, A. C.; Giambruno, R.; Weißer, J.; Májek, P.; Hofer, A.; Bigenzahn, J. W.; Superti-Furga, G.; Jessen, H. J.; Bennett, K. L. Identifying Kinase Substrates via a Heavy ATP Kinase Assay and Quantitative Mass Spectrometry. *Sci. Rep.* **2016**, *6* (1), 28107.
- (41) Li, Y.; Cross, F. R.; Chait, B. T. Method for Identifying Phosphorylated Substrates of Specific Cyclin/Cyclin-Dependent Kinase Complexes. *Proc. Natl. Acad. Sci. U.S.A.* **2014**, *111* (31), 11323–11328.
- (42) Collins, D. M.; Janardan, V.; Barneda, D.; Anderson, K. E.; Niewczas, I.; Taylor, D.; Qiu, D.; Jessen, H. J.; Lopez-Clavijo, A. F.; Walker, S.; Raghu, P.; Clark, J.; Stephens, L. R.; Hawkins, P. T. CDS2 Expression Regulates de Novo Phosphatidic Acid Synthesis. *Biochem. J.* 2024, 481 (20), 1449–1473.
- (43) Haas, T. M.; Mundinger, S.; Qiu, D.; Jork, N.; Ritter, K.; Dürr-Mayer, T.; Ripp, A.; Saiardi, A.; Schaaf, G.; Jessen, H. J. Stable Isotope Phosphate Labelling of Diverse Metabolites Is Enabled by a Family of 18O-phosphoramidites. *Angew. Chem., Int. Ed.* **2022**, *61*, 202112457.
- (44) Hofer, A.; Cremosnik, G. S.; Müller, A. C.; Giambruno, R.; Trefzer, C.; Superti-Furga, G.; Bennett, K. L.; Jessen, H. J. A Modular Synthesis of Modified Phosphoanhydrides. *Chem.—Eur. J.* **2015**, *21* (28), 10116–10122.
- (45) Qiu, D.; Gu, C.; Liu, G.; Ritter, K.; Eisenbeis, V. B.; Bittner, T.; Gruzdev, A.; Seidel, L.; Bengsch, B.; Shears, S. B.; Jessen, H. J. Capillary Electrophoresis Mass Spectrometry Identifies New Isomers of Inositol Pyrophosphates in Mammalian Tissues. *Chem. Sci.* 2023, 14 (3), 658–667.
- (46) Heijnen, J. J. Biosystems Engineering II, Linking Cellular Networks and Bioprocesses. *Adv. Biochem. Eng./Biotechnol.* **2010**, *121*, 139–162.
- (47) Wilson, M. S. C.; Bulley, S. J.; Pisani, F.; Irvine, R. F.; Saiardi, A. A Novel Method for the Purification of Inositol Phosphates from Biological Samples Reveals That No Phytate Is Present in Human Plasma or Urine. *Open Biol.* **2015**, *5* (3), 150014.
- (48) Wilson, M. S.; Saiardi, A. Inositol Phosphates Purification Using Titanium Dioxide Beads. *Bio-Protoc.* **2018**, *8* (15), No. e2959.
- (49) Qiu, D.; Eisenbeis, V. B.; Saiardi, A.; Jessen, H. J. Absolute Quantitation of Inositol Pyrophosphates by Capillary Electrophoresis Electrospray Ionization Mass Spectrometry. *J. Visualized Exp.* **2021**, 174..
- (50) Harmel, R. K.; Puschmann, R.; Trung, M. N.; Saiardi, A.; Schmieder, P.; Fiedler, D. Harnessing 13C-Labeled Myo-Inositol to Interrogate Inositol Phosphate Messengers by NMR. *Chem. Sci.* **2019**, 10 (20), 5267–5274.
- (51) Irvine, R. F.; Schell, M. J. Back in the Water: The Return of the Inositol Phosphates. *Nat. Rev. Mol. Cell Biol.* **2001**, 2 (5), 327–338.
- (52) Tsui, M. M.; York, J. D. Roles of Inositol Phosphates and Inositol Pyrophosphates in Development, Cell Signaling and Nuclear Processes. *Adv. Enzyme Regul.* **2010**, *50* (1), 324–337.
- (53) Chabert, V.; Kim, G.-D.; Qiu, D.; Liu, G.; Mayer, L. M.; Jamsheer K, M.; Jessen, H. J.; Mayer, A. Inositol Pyrophosphate Dynamics Reveals Control of the Yeast Phosphate Starvation Program Through 1,5-IP8 and the SPX Domain of Pho81. *eLife* **2023**, *12*, RP87956.

- (54) Dong, J.; Ma, G.; Sui, L.; Wei, M.; Satheesh, V.; Zhang, R.; Ge, S.; Li, J.; Zhang, T.-E.; Wittwer, C.; Jessen, H. J.; Zhang, H.; An, G.-Y.; Chao, D.-Y.; Liu, D.; Lei, M. Inositol Pyrophosphate InsP8 Acts as an Intracellular Phosphate Signal in Arabidopsis. Mol. Plant 2019, 12 (11), 1463-1473.
- (55) Riemer, E.; Qiu, D.; Laha, D.; Harmel, R. K.; Gaugler, P.; Gaugler, V.; Frei, M.; Hajirezaei, M.-R.; Laha, N. P.; Krusenbaum, L.; Schneider, R.; Saiardi, A.; Fiedler, D.; Jessen, H. J.; Schaaf, G.; Giehl, R. F. H. ITPK1 Is an InsP6/ADP Phosphotransferase That Controls Phosphate Signaling in Arabidopsis. Mol. Plant 2021, 14, 1864.
- (56) Auesukaree, C.; Tochio, H.; Shirakawa, M.; Kaneko, Y.; Harashima, S. Plc1p, Arg82p, and Kcs1p, Enzymes Involved in Inositol Pyrophosphate Synthesis, Are Essential for Phosphate Regulation and Polyphosphate Accumulation in Saccharomyces Cerevisiae. J. Biol. Chem. 2005, 280 (26), 25127-25133.
- (57) Pisani, F.; Livermore, T.; Rose, G.; Chubb, J. R.; Gaspari, M.; Saiardi, A. Analysis of Dictyostelium Discoideum Inositol Pyrophosphate Metabolism by Gel Electrophoresis. PLoS One 2014, 9 (1),
- (58) Desfougères, Y.; Portela-Torres, P.; Qiu, D.; Livermore, T. M.; Harmel, R. K.; Borghi, F.; Jessen, H. J.; Fiedler, D.; Saiardi, A. The Inositol Pyrophosphate Metabolism of Dictyostelium Discoideum Does Not Regulate Inorganic Polyphosphate (PolyP) Synthesis. Adv. Biol. Regul. 2022, 83, 100835.
- (59) Mitchell, R. A.; Lamos, C. M.; Russo, J. A. Mitochondrial-Catalyzed ATP Hydrolysis in Highly Enriched [180]H2O. Frequency Distributions of 18O-Labelled Pi Species. Biochim. Biophys. Acta, Bioenerg. 1980, 592 (3), 406-414.
- (60) Albert, C.; Safrany, T. S.; Bembenek, E. M.; Reddy, K. M.; Reddy, K. K.; Falck, J. R.; Bröcker, M.; Shears, B. S.; Mayr, W. G. Biological Variability in the Structures of Diphosphoinositol Polyphosphates in Dictyostelium Discoideum and Mammalian Cells. Biochem. J. 1997, 327 (2), 553-560.
- (61) Barker, C. J.; Wright, J.; Hughes, P. J.; Kirk, C. J.; Michell, R. H. Complex Changes in Cellular Inositol Phosphate Complement Accompany Transit through the Cell Cycle. Biochem. J. 2004, 380 (2), 465-473.
- (62) Hermes, J.; Kim, G.-D.; Liu, G.; Leo, M. G. D.; Mayer, A.; Jessen, H. j.; Timmer, J. The Break in the Cycle: Inositol Pyrophosphate Fluxomics Disentangled via Mathematical Modelling. bioRxiv 2025, 03.27.645712.
- (63) Kenyon, C. P.; Roth, R. L.; van der Westhuyzen, C. W.; Parkinson, C. J. Conserved Phosphoryl Transfer Mechanisms within Kinase Families and the Role of the C8 Proton of ATP in the Activation of Phosphoryl Transfer. BMC Res. Notes 2012, 5 (1), 131.
- (64) Lassila, J. K.; Zalatan, J. G.; Herschlag, D. Biological Phosphoryl-Transfer Reactions: Understanding Mechanism and Catalysis. Annu. Rev. Biochem. 2011, 80 (1), 669-702.
- (65) Dyson, J. M.; Fedele, C. G.; Davies, E. M.; Becanovic, J.; Mitchell, C. A. Phosphoinositide Phosphatases: Just as Important as the Kinases. Subcell. Biochem. 2012, 58, 215-279.
- (66) Goldbeter, A.; Koshland, D. E. An Amplified Sensitivity Arising from Covalent Modification in Biological Systems. Proc. Natl. Acad. Sci. U.S.A. 1981, 78 (11), 6840-6844.
- (67) Goldbeter, A.; Koshland, D. E. Energy Expenditure in the Control of Biochemical Systems by Covalent Modification. J. Biol. Chem. 1987, 262 (10), 4460-4471.
- (68) Samoilov, M.; Plyasunov, S.; Arkin, A. P. Stochastic Amplification and Signaling in Enzymatic Futile Cycles through Noise-Induced Bistability with Oscillations. Proc. Natl. Acad. Sci. U.S.A. 2005, 102 (7), 2310-2315.
- (69) Miller, C. A.; Beard, D. A. The Effects of Reversibility and Noise on Stochastic Phosphorylation Cycles and Cascades. Biophys. J. **2008**, 95 (5), 2183–2192.
- (70) Wykoff, D. D.; Rizvi, A. H.; Raser, J. M.; Margolin, B.; O'Shea, E. K. Positive Feedback Regulates Switching of Phosphate Transporters in S. Cerevisiae. Mol. Cell 2007, 27 (6), 1005-1013.

- (71) Vardi, N.; Levy, S.; Assaf, M.; Carmi, M.; Barkai, N. Budding Yeast Escape Commitment to the Phosphate Starvation Program Using Gene Expression Noise. Curr. Biol. 2013, 23, 2051.
- (72) Vardi, N.; Levy, S.; Gurvich, Y.; Polacheck, T.; Carmi, M.; Jaitin, D.; Amit, I.; Barkai, N. Sequential Feedback Induction Stabilizes the Phosphate Starvation Response in Budding Yeast. Cell Rep. 2014, 9 (3), 1122-1134.
- (73) Raser, J. M.; O'Shea, E. K. Control of Stochasticity in Eukaryotic Gene Expression. Science 2004, 304 (5678), 1811-1814. (74) Blind, R. D. Structural Analyses of Inositol Phosphate Second Messengers Bound to Signaling Effector Proteins. Adv. Biol. Regul. **2020**, 75, 100667.
- (75) Mallery, D. L.; Faysal, K. M. R.; Kleinpeter, A.; Wilson, M. S. C.; Vaysburd, M.; Fletcher, A. J.; Novikova, M.; Böcking, T.; Freed, E. O.; Saiardi, A.; James, L. C. Cellular IP6 Levels Limit HIV Production While Viruses That Cannot Efficiently Package IP6 Are Attenuated for Infection and Replication. Cell Rep. 2019, 29 (12), 3983-3996.
- (76) Obr, M.; Schur, F. K. M.; Dick, R. A. A Structural Perspective of the Role of IP6 in Immature and Mature Retroviral Assembly. Viruses 2021, 13 (9), 1853.
- (77) Renner, N.; Kleinpeter, A.; Mallery, D. L.; Albecka, A.; Faysal, K. M. R.; Böcking, T.; Saiardi, A.; Freed, E. O.; James, L. C. HIV-1 Is Dependent on Its Immature Lattice to Recruit IP6 for Mature Capsid Assembly. Nat. Struct. Mol. Biol. 2023, 30 (3), 370-382.
- (78) Macbeth, M. R.; Schubert, H. L.; VanDemark, A. P.; Lingam, A. T.; Hill, C. P.; Bass, B. L. Inositol Hexakisphosphate Is Bound in the ADAR2 Core and Required for RNA Editing. Science 2005, 309 (5740), 1534-1539.
- (79) Lee, W.-K.; Son, S. H.; Jin, B.-S.; Na, J.-H.; Kim, S.-Y.; Kim, K.-H.; Kim, E. E.; Yu, Y. G.; Lee, H. H. Structural and Functional Insights into the Regulation Mechanism of CK2 by IP6 and the Intrinsically Disordered Protein Nopp140. Proc. Natl. Acad. Sci. U.S.A. 2013, 110 (48), 19360-19365.
- (80) Sahu, S.; Gordon, J.; Gu, C.; Sobhany, M.; Fiedler, D.; Stanley, R. E.; Shears, S. B. Nucleolar Architecture Is Modulated by a Small Molecule, the Inositol Pyrophosphate 5-InsP7. Biomolecules 2023, 13 (1), 153.
- (81) Flood, D.; Lee, E. S.; Taylor, C. T. Intracellular Energy Production and Distribution in Hypoxia. J. Biol. Chem. 2023, 299 (9), 105103.
- (82) Imamura, H.; Nhat, K. P. H.; Togawa, H.; Saito, K.; Iino, R.; Kato-Yamada, Y.; Nagai, T.; Noji, H. Visualization of ATP Levels inside Single Living Cells with Fluorescence Resonance Energy Transfer-Based Genetically Encoded Indicators. Proc. Natl. Acad. Sci. U.S.A. 2009, 106 (37), 15651-15656.
- (83) Takaine, M.; Ueno, M.; Kitamura, K.; Imamura, H.; Yoshida, S. Reliable Imaging of ATP in Living Budding and Fission Yeast. J. Cell Sci. 2019, 132 (8), jcs230649.
- (84) Altschuler, S. J.; Wu, L. F. Cellular Heterogeneity: Do Differences Make a Difference? Cell 2010, 141 (4), 559-563.
- (85) Banfic, H.; Bedalov, A.; York, J. D.; Visnjic, D. Inositol Pyrophosphates Modulate S Phase Progression after Pheromone-Induced Arrest in Saccharomyces Cerevisiae. J. Biol. Chem. 2013, 288 (3), 1717-1725.
- (86) Tu-Sekine, B.; Kim, S. F. The Inositol Phosphate System—A Coordinator of Metabolic Adaptability. Int. J. Mol. Sci. 2022, 23 (12),
- (87) Laha, N. P.; Giehl, R. F. H.; Riemer, E.; Qiu, D.; Pullagurla, N. J.; Schneider, R.; Dhir, Y. W.; Yadav, R.; Mihiret, Y. E.; Gaugler, P.; Gaugler, V.; Mao, H.; Zheng, N.; von Wirén, N.; Saiardi, A.; Bhattacharjee, S.; Jessen, H. J.; Laha, D.; Schaaf, G. INOSITOL (1,3,4) TRIPHOSPHATE 5/6 KINASE1-Dependent Inositol Polyphosphates Regulate Auxin Responses in Arabidopsis. Plant Physiol. **2022**, 190 (4), 2722–2738.
- (88) Kim, G.-D.; Qiu, D.; Jessen, H. J.; Mayer, A. Metabolic Consequences of Polyphosphate Synthesis and Imminent Phosphate Limitation. mBio 2023, 14 (3), e00102-e00123.

(89) Azevedo, C.; Burton, A.; Bennett, M.; Onnebo, S. M. N.; Saiardi, A. Synthesis of InsP7 by the Inositol Hexakisphosphate Kinase 1 (IP6K1). *Methods Mol. Biol.* **2010**, *645*, 73–85.